BACTERIAL HERD AND SOCIAL IMMUNITY TO PHAGES

by

Pavel Payne

November, 2016

A Thesis
Presented to the Faculty of the Graduate School of the
Institute of Science and Technology Austria, Klosterneuburg, Austria
in Partial Fulfillment of the Requirements for the Degree
Doctor of Philosophy

Supervisor: Jonathan P. Bollback, IST Austria, Klosterneuburg, Austria

Signature: [redacted]

Co-supervisor: Nicholas H. Barton, IST Austria, Klosterneuburg, Austria

Signature: [redacted]

Committee Member: Thomas Flatt, University of Lausanne, Switzerland

Signature: [redacted]

Committee Member: Calin Guet, IST Austria, Klosterneuburg, Austria

Signature: [redacted]

Defense Chair: Gašper Tkačik, IST Austria, Klosterneuburg, Austria

Signature: [redacted]

I hereby declare that this dissertation is my own work, and it does not contain other peoples work without this being so stated; and this thesis does not contain my previous work without this being stated, and that the bibliography contains all the literature that I used in writing the dissertation, and that all references refer to this bibliography.

I declare that this is a true copy of my thesis, including any final revisions, as approved by my thesis committee, and that this thesis has not been submitted for a higher degree to any other University or Institution.

Signature: 

Pavel Payne
February, 2017

Biographical Sketch

Pavel Payne was born in 1985 in Prague, where he grew up and obtained his undergraduate education at the Charles University. In 2009 he received his Bachelor's degree in Ecology and Environmental Protection. In 2011 he finished his Master studies in Theoretical and Evolutionary Biology with a defence of his Master Thesis entitled The Role of Genetic Variability in Speciation. In the same year he started his PhD studies at IST Austria.

List of Publications

Acknowledgments

I am very much obliged to many people who supported me during my doctoral studies, but particularly I would like to thank Jon Bollback and Nick Barton for their guidance, support, patience, and for letting me examine and study topics beyond the actual topic of my PhD research. I am also particularly thankful to Calin Guet for his occasional advice on experimental issues and for his boundless encouragement and support when hurdles to my research seemed insurmountable.

It has been an enriching experience to cooperate with Lukas Geyrhofer, who contributed tremendously to the modelling of bacterial herd immunity. I would also like to thank Remy Chait, who helped me to establish various experimental setups necessary to obtain precious data.

Besides those mentioned above, I am grateful to all current and former members of both the Bollback and Barton group for the friendly and creative environment they created and their help with many experimental and theoretical issues.

I am also very grateful to my external committee member Thomas Flatt for his time and the feedback he gave me both on the PhD thesis proposal and more importantly on the final thesis.

Furthermore I very much appreciated the interdisciplinary atmosphere of IST Austria and the support from our group assistants Elisabeth Hacker, Nicole Hotzy, Julia Asimakis, Christine Ostermann and Jerneja Beslagic.

Finally I thank Táňa for her love and patience throughout the whole journey of my doctoral studies, and my parents and siblings for their continuous support.

Abstract

Bacteria and their pathogens – phages – are the most abundant living entities on Earth. Throughout their coevolution, bacteria have evolved multiple immune systems to overcome the ubiquitous threat from the phages. Although the molecular details of these immune systems' functions are relatively well understood, their epidemiological consequences for the phage-bacterial communities have been largely neglected. In this thesis we employed both experimental and theoretical methods to explore whether herd and social immunity may arise in bacterial populations. Using our experimental system consisting of *Escherichia coli* strains with a CRISPR based immunity to the T7 phage we show that herd immunity arises in phage-bacterial communities and that it is accentuated when the populations are spatially structured. By fitting a mathematical model, we inferred expressions for the herd immunity threshold and the velocity of spread of a phage epidemic in partially resistant bacterial populations, which both depend on the bacterial growth rate, phage burst size and phage latent period. We also investigated the potential for social immunity in *Streptococcus thermophilus* and its phage 2972 using a bioinformatic analysis of potentially coding short open reading frames with a signalling signature, encoded within the CRISPR associated genes. Subsequently, we tested one identified potentially signalling peptide and found that its addition to a phage-challenged culture increases probability of survival of bacteria two fold, although the results were only marginally significant. Together, these results demonstrate that the ubiquitous arms races between bacteria and phages have further consequences at the level of the population.

Table of Contents

List of Tables

List of Figures

List of Abbreviations

Abi Abortive infection

bp Basepair

BREX Bacteriophage-exclusion

CaCl Calcium chloride

Cas CRISPR associated proteins

CDS Coding sequence

CFU colony forming unit

conc. Concentration

CRISPR Clustered regularly interspaced short palindromic repeats

DNA Deoxyribonucleic acid

Gly Glycine

H Herd immunity threshold

h Hours

HCl Hydrogen chloride

hpi Hours post inoculation

L Luminosity

LB Luria-Bertani broth

LC-MS Liquid chromatography–mass spectrometry

MHC Major histocompatibility complex

ml Milliliter

mM Millimolar

MOI Multiplicity of infection

μg Microgram

μl Microliter

μM Micromolar

nm Nanometer

nt Nucleotide

OVN Overnight

Pcrap Potential CRISPR activating peptide

pfu Plaque forming units

R_0 Basic reproduction number

RM Restriction–modification

RNA Ribonucleic acid

RNAi RNA interference

S Fraction of susceptible individuals

sORF Short open reading frame

TF Transcription factor

Tris Tris(hydroxymethyl)aminomethane

UTR 5’ untranslated region

For a list of all variables and parameters used in the herd immunity model see Table 2.4 in Supplementary information (Section 2.6.1)

1 Introduction

Bacteria and Archaea are the most abundant cellular organisms on Earth ($> 10^{30}$ individuals globally) (Whitman *et al.*, 1998) and the most diversified kingdoms on the tree of life (Hug *et al.*, 2016). They are essential for virtually all biogeochemical processes and inhabit literally every corner of our planet (Prosser *et al.*, 2007). However abundant these organisms are, they are outnumbered about ten fold by their viral pathogens called bacteriophages (Abedon, 2008) or phages[1].

Phages have evolved a variety of life history strategies to reproduce in their prokaryotic hosts. Phages capable of temperate life cycle and filamentous phages can form long-term associations with their hosts in a process called lysogeny and pseudolysogeny, respectively (Koskella and Brockhurst, 2014). Phages with a purely lytic life cycle require lysis of the cell to reproduce, thus they are obligate killers of their hosts (Hyman and Abedon, 2012). While temperate and filamentous phages are not necessarily detrimental to the host, and eventually may even alter the host phenotype in a beneficial way (e.g. provide antibiotic resistance or toxin production (Brüssow *et al.*, 2004; Waldor and Mekalanos, 1996)), purely lytic phages pose a significant threat to the hosts and represent a strong selection pressure. In response, bacteria have evolved a number of immune mechanisms to defend themselves and many of these mechanisms have been understood in a great detail at the molecular level. In the next section we briefly review the bacterial immune mechanisms discovered up to now and explain how they function.

[1] For clarity, throughout this thesis we will stick to the term 'phage' and its plural form 'phages', as has been established in a majority of the literature (Ackermann, 2011).

1.1 Bacterial immune systems

Bacteria defend themselves against phages in a variety of ways. These defences can be divided into four classes according to the mechanisms of their function: (i) preventing phage adsorption, (ii) preventing phage DNA entry, (iii) abortive infection systems and (iv) phage nucleic acid degradation (Labrie *et al.*, 2010).

Prevention of phage adsorption (i) occurs in a variety of ways including mutations in genes that code for adsorption sites of phages (Luria and Delbrück, 1943), blocking of phage receptors (Nordström and Forsgren, 1974), production of extracellular matrix (Blumenthal and Cheng, 2002), and competitive inhibitors (Destoumieux-Garzón *et al.*, 2005).

Another class of bacterial defence is the prevention of phage DNA entry (ii) encoded by genes often found in prophages to provide superinfection exclusion (Lu and Henning, 1994). This suggests that they have evolved as a result of interactions between different phages rather than between phage and host.

The third class of immune responses are abortive infection (Abi) systems (iii), which are 'altruistic' systems that limit phage replication by the host's suicide, preventing further spread of the phage through the bacterial population (Chopin *et al.*, 2005).

The last class of immune responses are those that target phage genomes for degradation (iv). The first immune systems described, and undoubtedly the most common, are the host restriction-modification (RM) systems (Oliveira *et al.*, 2014), which cleave foreign DNA at specific 4-8nt long sites; self-nonself recognition occurs via methylation of sites in the host genome (Blumenthal and Cheng, 2002). A similar but less common immune system is the recently discovered bacteriophage-exclusion (BREX) system (Goldfarb *et al.*, 2015), which inhibits phage replication via some other, yet unknown, mechanism that seems not to involve foreign DNA cleavage. Some authors also consider so called Argonaute-based RNAi-like system (Swarts *et al.*, 2014) as a potential phage RNA interference mechanism (Kaya *et al.*, 2016). The last of the known foreign DNA degrading immune systems are the CRISPR/Cas (clustered regularly interspaced short palindromic repeats)

systems. These systems cleave foreign DNA based on a 26-72nt long stretch of the phage genome (spacer) that has been previously incorporated into a special 'immune memory' locus, with sequence specific self-nonself recognition (Sorek *et al.*, 2013).

The molecular mechanisms and functional details of some of these bacterial immune systems have been repurposed as extremely powerful tools for DNA manipulations, such as restriction enzymes (Loenen *et al.*, 2014) and the CRISPR/Cas9 genome editing systems (Doudna and Charpentier, 2014).

1.2 Bacteria–phage coevolution

Given the abundance of bacteria and phages and the arsenal of immune systems bacterial hosts have evolved, the question what consequences interactions between bacteria and phages can have on their ecology and evolution has been of an interest to many microbial evolutionary ecologists. The effects of these interactions have been examined in a number of laboratory experiments focusing on bacteria–phage coevolution, a process defined as continuous adaptation and counter-adaptation between interacting species in a community (Van Valen, 1973; Janzen, 1980; Stern and Sorek, 2011), (for a review see Koskella and Brockhurst, 2014). It has been shown that phages can influence competition among bacterial strains and species (e.g., Bohannan and Lenski, 2000b,a; Koskella *et al.*, 2012) maintain bacterial diversity (e.g., Buckling and Rainey, 2002b,a) and that the phages evolve their infectivity range (Hall *et al.*, 2011).

A common scheme of bacteria-phage coevolutionary experiments is a long term coculturing of bacteria and phages with periodical quantification of various factors such as phage and bacterial concentrations and diversities, evolution of bacterial resistance, and evolution of phage infectivity. These experiments allow for observations of the outcomes mentioned above, but it is often difficult to assess whether the processes responsible for these outcomes can be attributed to ecological, microevolutionary or coevolutionary dynamics (Koskella and Brockhurst,

2014).

It has been shown that maintenance of bacterial host diversity and their coexistence with the phage can be ascribed to spatial refuges in unshaken flasks (Schrag and Mittler, 1996), costs of resistance (Bohannan *et al.*, 2002), heterogeneity in the bacteria and phage populations, and the availability of resources (Chao *et al.*, 1977; Levin *et al.*, 1977; Lenski and Levin, 1985; Bohannan and Lenski, 1997, 1999, 2000b). Coexistence of phages and bacteria, however, has been shown to be possible even in cultures without spatial refuges available (Lenski, 1988; Schrag and Mittler, 1996), whereas the mechanisms allowing the bacteria and phage to coexist in these environments seemed rather unclear (Lythgoe and Chao, 2003).

Interestingly, none of the approaches employed in the studies mentioned above has taken into account processes happening at the border of ecology and microevolution – host–pathogen epidemiology. In the past decades, epidemiologists have developed a large body of theory addressing questions of how pathogens spread and persist and the dynamics of immune and susceptible individuals in populations. Adopting these approaches for bacteria–phage systems can allow us to disentangle at which level the processes such as coexistence of bacteria and phages and maintenance of bacterial diversity happen, and even quantify their effects and dynamics.

The main epidemiological processes playing an important role in host–pathogen interactions are herd and social immunity. Therefore, investigation whether and how herd and social immunity may contribute to the dynamics in bacteria–phage systems can substantially enhance our understanding of the roles of various ecological, microevolutionary and coevolutionary processes in these microbial communities.

1.3 Herd immunity

One important emerging property of immune competent populations, which has an impact on their ecology and evolution, is herd immunity. The term herd immunity has a variety of meanings (Fine *et al.*, 2011) but in its most general definition, herd immunity is a phenomenon when a resistant fraction of a population reduces the probability of transmission of a pathogen within the susceptible fraction of the population. Thus, it determines whether and how a pathogen can spread through a partially resistant population.

The dynamics of pathogen spread through host populations depends on many factors such as the virulence of the pathogen, modes of transmission, contact rate, the mode of immunity of the hosts in the population, and the frequency of resistant and susceptible hosts. The properties of the host-pathogen system (i.e., virulence, means of transmission, and contact rate) can be integrated into one compound parameter, R_0, which is the basic reproduction number of the pathogen. R_0 describes the fitness of the pathogen in a fully susceptible population and can be defined as the number of new cases of a disease initiated by one infected individual. The fraction of resistant hosts in the population then determines whether a pathogen will spread and can be described by a simple formula that characterizes the threshold at which herd immunity will occur,

$$H = \frac{R_0 - 1}{R_0} \, ,$$

Thus, if the fraction of resistant hosts is higher than the herd immunity threshold, the resistant individuals provide indirect protection to the susceptible hosts in the population, i.e., they provide them with herd immunity (Fig. 1.3 and Fig. 1.3).

Herd immunity has mainly been studied in human and animal populations (Fine, 1993) with respect to individual adaptive immunity (Pancer and Cooper, 2006). Adaptive immunity refers to antigen-specific immune response, which provides an immune memory of resistance after a recovery from a disease or after vaccination. It has been shown that unless the resistant fraction of a population is

forced by vaccination to stay above the herd immunity threshold, the incidence of the disease cycles around the birth rate and the number of resistant individuals cycles around the herd immunity threshold. In other words, herd immunity can generate frequency dependent selection on resistance and maintain polymorphism for immunity in the population (Fine, 1993).

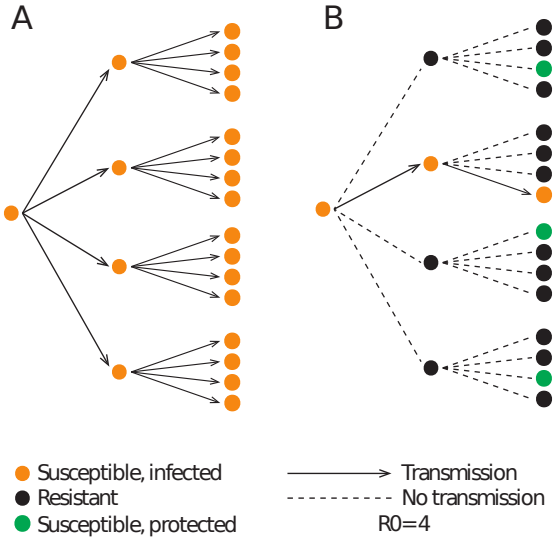

Figure 1.1: Illustration of the transmission of a pathogen with a basic reproduction number $R_0 = 4$ over three generations. A) Fully susceptible population: Single introduced case leads to 4 cases and then to 16 cases, so the number of infected individuals increases exponentially. B) Partially resistant population: ¾ of the population is resistant, thus a single introduced case leads to only one successful transmission per generation, i.e., one another infected individual. If more than ¾ of the population are resistant, the pathogen incidence will decline over time, because the herd immunity threshold, H, would be exceeded.

As we have mentioned above, bacteria may possess many immune systems against their abundant pathogens, phages, and one of the systems, namely CRISPR/Cas, shows a high functional analogy to vertebrate adaptive immunity. Therefore, it is reasonable to expect that herd immunity may also occur in bacterial populations which are only partially resistant.

1.4 Social immunity

Another interesting property related to resistance of a population to a pathogen is social immunity. As organisms often live in populations where individuals within

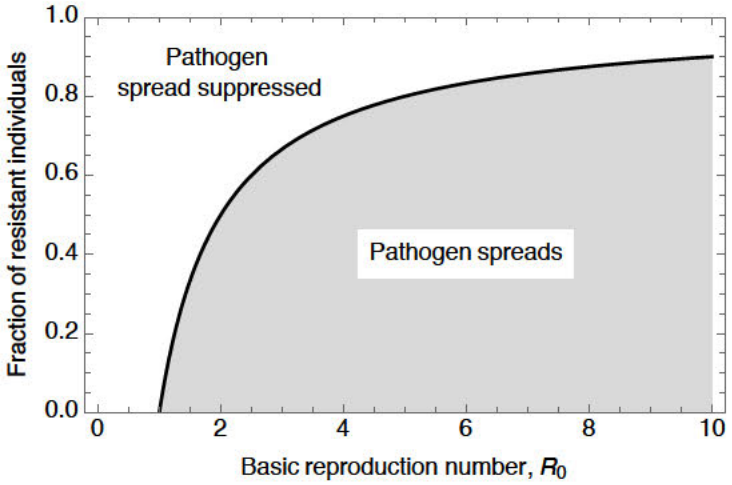

Figure 1.2: Graphical representation of the herd immunity threshold. On the x-axis is the fitness of the pathogen represented by the basic reproduction number, on the y-axis the fraction of resistant individuals in the population. Herd immunity threshold is represented by the black curve. If the fraction of resistant individuals in the population is below the herd immunity threshold, the pathogen will spread in the population (shaded area), if the fraction of resistant individuals in the population is above the herd immunity threshold, the pathogen spread is suppressed.

sub-populations are more closely related than individuals between sub-populations, pathogens are more likely to spread within the subpopulations because of the reduced genetic diversity that may facilitate their spread (King and Lively, 2012). As a response, many animal species have evolved behaviours which are not necessarily beneficial for the acting individual but reduces the pathogen or parasite load in the sub-population. This phenomenon has been called social immunity and can be defined as 'any collective and personal mechanism that has emerged and/or is maintained at least partly due to the anti parasite defence it provides to other group members' (Meunier, 2015).

It is important to note that social immunity is often conditional on the transmission of information describing the health status of the infected individual to healthy individual(s), or by recognition of the symptoms by the acting individuals.

Bacteria often live in structured environments and produce clonal offspring, *i.e.*, live in sub-populations with very high relatedness. Also, bacteria are capable of transmitting information from one individual to another using small signalling pheromones and respond to the signal usually in a concerted manner, which is

often called quorum sensing (Miller and Bassler, 2001). Since these two facts are prerequisites for social immunity, it suggests that bacteria may also be capable of mounting a social immune response to a phage attack.

1.5 Thesis aims

Although it seems reasonable to expect that bacteria may exhibit both herd and social immunity, any direct evidence of the existence of these phenomena is still lacking. In order to explore whether and how herd and social immunity may occur in bacterial populations, we employed both experimental methods and mathematical modelling. Specifically, the aims of this thesis are to:

1. set up an experimental system consisting of susceptible and resistant bacterial strains and their phage, which allows us to explore whether herd immunity emerges in bacterial populations;

2. investigate how the effect of herd immunity changes in habitats with or without a spatial structure;

3. construct a mathematical model and measure as many parameters as possible to identify the crucial factors determining the effect of herd immunity to phages in bacteria;

4. examine the means of bacterial communications which can be linked to immunity and experimentally evaluate candidate pheromones potentially mediating bacterial social immunity.

Besides our interest in the role of herd and social immunity in bacteria–phage communities, such experimental systems may also allow for convenient testing of general epidemiological hypotheses, which can be further applied to non-microbial host–pathogen systems. In fact, there is a call by epidemiologists for such analogous model systems which can be informative about traditional vertebrate host–pathogen systems (Babayan and Schneider, 2012).

2 CRISPR-based Herd Immunity Limits Phage Epidemics in Bacterial Populations

Mathematical modelling contained in this chapter has been done in cooperation with Lukas Geyrhofer (Technion – Israel Institute of Technology, Haifa, Israel) who has encoded the model and performed most of the analyses.

2.1 Abstract

Pathogens are a driving force in evolution giving rise to a diversity of host immune defenses. In order for a pathogen to spread in a population a sufficient number of individuals must be susceptible to infection as resistant individuals can prevent the spread of a pathogen to susceptible individuals in a process known as herd immunity. While herd immunity has been extensively studied in vertebrate populations, little is known about its role, if any, in the dynamics between bacteria and their phage pathogens. Here we explore the dynamics of T7 phage epidemics in structured and unstructured *Escherichia coli* populations consisting of differing mixtures of susceptible and resistant individuals harboring CRISPR immunity to the phage. Using both experiments and mathematical modelling we describe the conditions under which herd immunity arises in bacterial populations. Notably, the effects of herd immunity depend strongly on the presence of spatial structure in the population, the bacterial growth rate, and phage replication rate. In addition,

we provide a model system for exploring general epidemiological principles. Our findings suggest that studies of phage-bacterial communities should take herd immunity into consideration and its impact on the long term evolutionary and ecological dynamics.

2.2 Introduction

The term “herd immunity” has a variety of meanings (see Fine *et al.*, 2011). Here, we use it in its general meaning as a phenomenon where a resistant fraction of a population reduces the probability of transmission of a pathogen among susceptible individuals. Historically, before large-scale vaccination programs, acquired immunity occurred through exposure to the pathogen, which often led to cycles of disease incidence over time (Fine, 1993). After efficient vaccines were developed and large-scale vaccination began, immunisation of a high proportion of individuals in populations prevented epidemics of many pathogens. One of the best known observations of herd immunity was the worldwide vaccination program to eradicate smallpox between 1959 and 1977 (Fenner, 1993). On the heels of this success, other vaccination programs were developed and applied in an attempt to control other pathogens, e.g., poliomyelitis, measles, rubella, mumps, diphtheria, tetanus, and tuberculosis (Anderson and May, 1985b; Anderson, 1995; Fine, 1993). Herd immunity has been studied mostly in vertebrates, including foxes (Jeltsch *et al.*, 1997), birds (Boven *et al.*, 2008; Meister *et al.*, 2008) , and cattle (Mariner *et al.*, 2012), but also in some invertebrates (Konrad *et al.*, 2012; Wang *et al.*, 2013).

Concurrent with advances in vaccination programs, mathematical theories aiming at discovering the principles underlying herd immunity were developed. The first theory of herd immunity was proposed by Hamer (1906), showing that the number of transmission events of measles was a function of the number of susceptible individuals in the population. This theory has become known as the epidemiologic ‘law of mass action’ by analogy to the rate of a chemical reaction

as a product of the initial concentrations of the reagents (Soper, 1929). This approach led to formalisation of a general theory of herd immunity, with a central parameter R_0, which can be linked to the 'law of mass action theory' as being the number of further infections after a single case has been introduced into a fully susceptible population (for a historical review of R_0 see (Heesterbeek, 2002)). R_0 thus describes the fitness of the pathogen, which determines the spreading potential of an infection in a population and is a function of the biological mechanisms of transmission and the rate of contact between individuals. This leads to a critical condition, the herd immunity threshold,

$$H = \frac{R_0 - 1}{R_0} \,, \tag{2.1}$$

which determines the minimum fraction of resistant individuals needed to halt an epidemic (Grassly and Fraser, 2008). A simple derivation for (2.1) is presented in Box 1.

Although H tells us the fraction of a population that needs to be vaccinated, it does not explicitly describe the mechanisms of transmission or the rate of contacts in the population. In other words it is a 'black box' parameter, which is influenced by the biological details of the pathogen and of the population itself. Many theoretical studies have addressed the influence of some of these factors on R_0, in particular maternal immunity (Anderson and May, 1992), age at vaccination (Anderson and May, 1982; Nokes and Anderson, 1988), age related or seasonal differences in contact rates (Schenzle, 1984; Anderson and May, 1985a; Yorke *et al.*, 1979), social structure (Fox *et al.*, 1971), geographic heterogeneity (Anderson and May, 1984; Lloyd and May, 1996; Real and Biek, 2007), and the general underlying contact network of individuals (Ferrari *et al.*, 2006).

2.2.1 Herd immunity in bacteria

As is evident from studies of herd immunity in vertebrates, when and how herd immunity occurs is strongly host and pathogen specific. Therefore, the question

Herd immunity in liquid culture can be explained with a simple, but compelling, intuition. The number of additional infections originating from a single infected host is usually denoted R_0 in the epidemological literature. If one infection produces at least one more infected host, $1 < R_0$, the pathogen will spread. In our case, we have a mixture of immune and susceptible hosts, and S indicates the fraction of susceptible individuals.
For well mixed populations, that do not exhibit any spatial structure, we can estimate the herd immunity threshold H via a straightforward argument: With probability S the pathogen infects a susceptible host and produces R_0 additional pathogens, while with probability $1 - S$ a pathogen encounters a resistant host, which can terminate the infection. Again, if on average at least one additional infection is generated from a single infected host, the epidemic will spread. Mathematically, this can be expressed in the condition $1 < SR_0$.
Usually, the herd immunity threshold H is defined as the fraction of *resistant* hosts (instead of the fraction of *susceptible* hosts). This leads to $H = 1 - S_c$, where S_c is the critical fraction of susceptible individuals that allows an infection to barely spread, i.e., an infection produces exactly one offspring. Inverting the resulting condition, $1 = (1 - H)R_0$, yields immediately the expression,

$$H = \frac{R_0 - 1}{R_0} \, ,$$

which we also stated in the main text, (2.1). Additionally, one can adopt a dynamical interpretation for this expression: Over time, the fraction of susceptible individuals will decline further, and pathogen encounter more resistant cells, leading to a increasingly immune population.
In the context of phages infecting bacterial populations, R_0 is as a first approximation simply the burst size of phages β. However, even in liquid culture, this number R_0 is modified by additional interactions between host, pathogen, and environment.

Box 1: Basic principles of herd immunity.

to what extent patterns of herd immunity apply also to the microbial world is still unanswered. Bacteria and phages are the most abundant organisms on Earth (Whitman *et al.*, 1998; Abedon, 2008). Thus, investigating their interaction can provide clues for understanding their impact on other ecological processes, but also for the dynamics of infectious diseases in general. The advantage of using bacteria and phages as a model system is that theoretical predictions can be directly tested under controlled laboratory conditions. In following sections we briefly discuss bacterial immune systems with respect to their potential to provide herd immunity against virulent phages.

2.2.1.1 Bacterial immune systems and their potential for herd immunity

Bacteria have multiple defence mechanisms against phages. These mechanisms target various stages of the phage life cycle. The early defence mechanisms include prevention of phage adsorption, e.g., by mutations in genes that code for adsorption sites of phages (Luria and Delbrück, 1943), blocking of phage receptors (Nordström and Forsgren, 1974), production of an extracellular matrix (Hammad, 1998; Sutherland *et al.*, 2004), or of competitive inhibitors (Destoumieux-Garzón *et al.*, 2005). Besides these avoidance mechanisms, bacteria have also evolved various endogenous immune systems that mostly restrict foreign DNA injected into the cell by a phage. These immune systems include so called innate immune systems: restriction-modification (RM) (Blumenthal and Cheng, 2002), abortive infection (Abi) (Chopin *et al.*, 2005), argonaute-based RNAi-like (Swarts *et al.*, 2014), and bacteriophage-exclusion (BREX) system (Goldfarb *et al.*, 2015), and an adaptive immune system called CRISPR/Cas (clustered regularly interspaced short palindromic repeat) (Sorek *et al.*, 2013).

In order to provide significant herd immunity, the immune system must prevent further spread of the pathogen, i.e., provide a 'sink' for the infectious particles, and the population must be polymorphic for immunity.

From the defence mechanisms listed above, only RM, BREX, argonaute-based RNAi-like, and the CRISPR/Cas systems degrade foreign phage DNA after it is injected into the cell, thus providing a stable 'sink' for the phage. Bacterial populations may certainly be polymorphic for the innate immunity via a presence/absence (or loss of function) polymorphism. The CRISPR/Cas system, in addition to this possibility of presence/absence polymorphism, is capable of adaptive acquisition of new spacers (Barrangou *et al.*, 2007), which can generate another level of polymorphism for immunity to different phages (Horvath *et al.*, 2008). Although the exact rate of spacer acquisition is poorly known and varies with experimental conditions (Levin *et al.*, 2013), the probability that a population would be polymorphic for the CRISPR-based immunity is likely to be higher than for any other immune response mentioned above.

In addition to immune system-specific factors, the fecundity of a phage also depends strongly on the physiology of the host bacterium (Hadas *et al.*, 1997), and the underlying effective contact network which may vary greatly in bacterial populations depending on the details of their habitat. Thus, R_0 will vary depending on the physiological state of the bacteria and the mobility of the phage in the environment through passive diffusion and movement of infected individuals. Taken together these details call into question the applicability of the traditional models of herd immunity in vertebrates to phage-bacterial systems and requires both experimental investigation and the development of models that take into account the details of phage-bacterial systems.

2.2.2 Our experimental system

In order to examine under which conditions herd immunity may arise in phage-bacterial communities, we constructed an experimental system in which we could explore the dynamics of phage spread in non-structured and structured populations consisting of phage-susceptible and phage-resistant individuals. The experimental system consists of *Escherichia coli* strains, one of them possessing a CRISPR-based immunity to the T7 phage. In order to be able to monitor the spread of the epidemic and assess the impact of the CRISPR system on herd immunity of the population, we constructed the resistant strain so that once a resistant cell is infected by a phage the cells' growth is halted. However, cells still function as a 'sink' to the phage. Thus, we rule out the possibility that resistant bacteria overgrow patches already wiped out by phages. Moreover, it allows us to focus solely on the dynamics of phage spread in a 'naive' population.

In addition, we have developed and analysed a spatially explicit model of our experimental system in order to determine which parameters are crucial for the population to exhibit herd immunity.

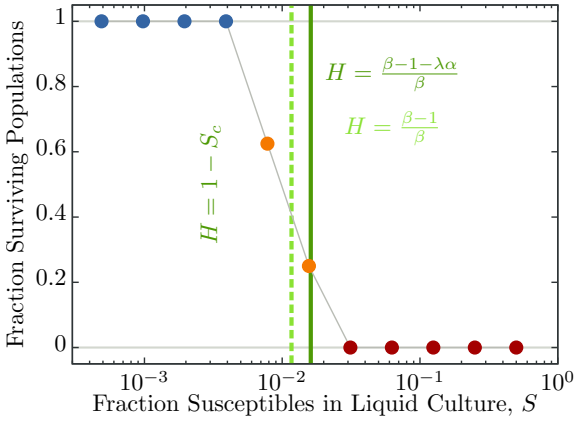

Figure 2.1: **Percentage of surviving populations at $18\,h$ after inoculation.** Initially, the bacterial populations with various fractions of susceptible and resistant bacteria is infected with ~ 50 phages, corresponding to a "multiplicity of infection" (MOI) $\sim 10^{-4}$. Each population composition is replicated 16 times. The predicted herd immunity threshold $H = 1 - S_c$ coincides with the population composition where the populations start to survive the phage infection, The dashed light green curve indicates H as in (2.7), which depends only on the phage burst size β. The solid dark green line shows the prediction (2.8), which also includes a correction due to time scales given by the latency time λ and the bacterial growth rate α.

2.3 Results

2.3.1 Herd immunity in spatially unstructured liquid cultures

To understand the influence of spatial population structure, or lack thereof, we conducted a set of experiments in a well mixed liquid environment consisting of differing proportions of resistant and susceptible individuals. Under these conditions, with no spatial structure, all 16 replicate populations survive a phage epidemic when 99.6% of individuals are resistant, 4 out of 16 replicate populations survive when 98.4% of individuals are resistant, and all populations went extinct when the proportion of resistant individuals drops below 96.9% (see Figure 2.1). Such a simple dilution scheme thus provides a first clue for the value of the herd immunity threshold H, and we can estimate R_0 of the phage in this environment as ranging between 32 and 256. However, utilising our theoretical approach (below), we can refine this estimate by using more accessible measurements. After all, each population in such a dilution series has to be replicated several times (we used 16 replicates) and each set of parameters only can provide a

limiting boundary for the actual value.

Phage fecundity plays a major role in determining a viable population composition of susceptible and resistant bacteria. This can be seen directly by decreasing the nutrient concentration in the media, which entails slower bacterial growth. In turn, phages that depend on bacterial metabolism grow slower, too, affecting herd immunity. Indeed, we observe a substantial increase in the critical fraction of susceptible cells, such that the bacterial populations survive a phage infection (see Fig. 2.3). Additional support is provided by results in Fig. 2.5 and Tables 2.3 and 2.2, which list measured growth rates for phages and bacteria in different conditions, respectively.

2.3.2 Herd immunity in spatially structured surface populations

In order to better understand what role, if any, spatial structure plays in herd immunity we conducted a set of experiments in a spatially structured semi-solid environment – on soft agar plates. The approach employed here is a much more fine grained measure of herd immunity, compared to the binary alive-dead outcomes for the populations in liquid culture. On plates, phages can spread radially from a single infection and the radius of the plaque provides an easy measure that can quantify the influence of the population composition of susceptible and resistant bacteria. During the first approximately 12 hours of the experiments, bacteria in the soft agar layer grow exponentially (Fig. 2.5A) and the plaques also spread fast because the phage burst size on exponentially growing cells is large (85). After about 12 hours the bacterial growth starts slowing down because they deplete available nutrients in the agar and as a consequence, also the burst sizes decrease dramatically (to 3 on non-growing cells). This reduction in burst size results in a dramatic decrease in plaque growth or its cessation.

We observed that final plaque sizes were significantly reduced already with 10% of resistant cells in the population (Fig. 2.2). In order to determine the effect of resistant cells in the exponential phase of their growth, we analysed velocities

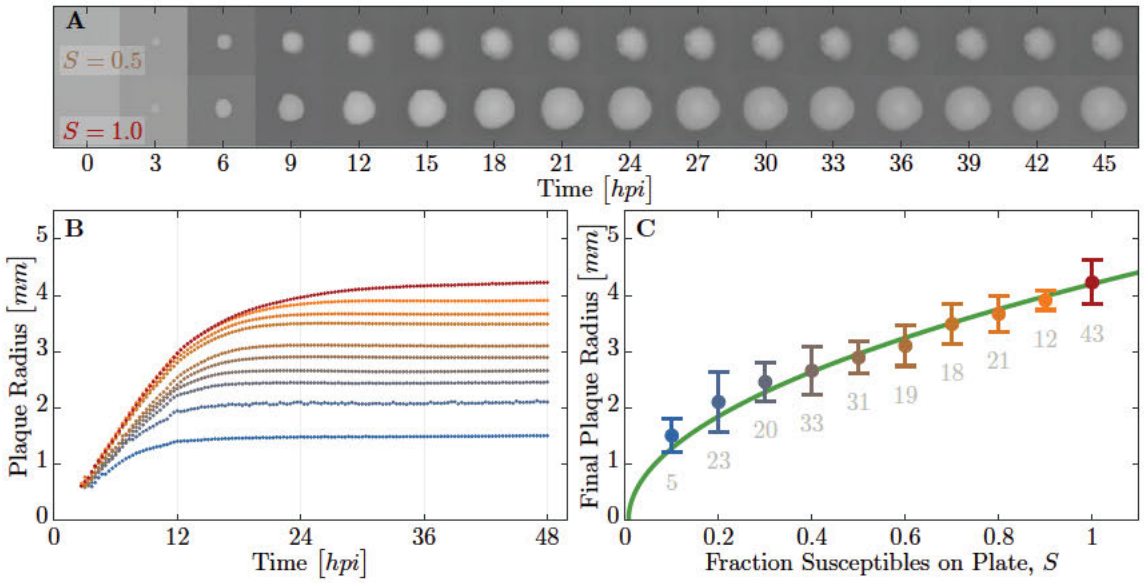

Figure 2.2: **Growing phage on a bacterial lawn on agar plates.** (A) Plaque sizes sampled throughout 48 hours for populations with 50% susceptible cells and a control with 100% susceptible cells. (B) Averaged increase in plaque size measured from the area of cleared bacterial lawn over time, assuming a circular area. Colours indicate the different fraction of susceptible individuals, with identical colouring as in (C). Note the distinct two phases of phage growth: initially, phage grow fast with exponentially growing bacteria. After nutrients are depleted (after time T_{depl}) the expansion of phages stops, and plaque radius stays at a constant value when the population contains resistant bacteria. Thus, plaque radius is changed already for even a very small fraction of resistant bacteria. (C) Final plaque radius from (B) together with the predicted plaque radius r in our model (see Eq. (2.13), green line). Grey numbers indicate the number of plaques used to compute averages.

of spread of the plaques between 0 and 24 hours post inoculation (hpi), and found that the velocity is significantly reduced after $15\,hpi$ when the population consists of 10% of resistant cells (P-value < 0.045). When the fraction of resistant cells is further increased, the velocity difference is significant at earlier and earlier stages of the experiments ($11.3\,hpi$ for 20% resistant, $5.7\,hpi$ for 30% resistant) and when the resistant fraction reaches 40%, the difference in velocity of spread becomes significant right after the plaques become detectable in our experimental setup (Fig. 2.7).

The dynamics of the system on soft agar plates is influenced by additional factors. Movement of phages is characterised with a single diffusion constant D. Phage adsorption should be considered different, too: The additional spatial dimension imposes a particular contact network between phages and bacteria, which are not entirely random encounters. In order to determine the extent to which these parameters play a role, we conducted additional experiments to estimate their values. In particular, we inferred the diffusion constant D by measuring how a fluorescence signal indicating phage presence spreads without bacteria (see section 2.5.7). Although bacteria may lower the diffusion constant when they reach high densities, we assume the spread of the phage through the bacterial population would not be substantially affected because it is likely dominated by the phage growth parameters and the fraction of resistant individuals in the population. Therefore, even if the diffusion constant changes, it probably does not influence the overall dynamics in a detectable way. Moreover, we again used the independent estimates for phage growth and bacterial growth in various environmental conditions. These results on growth are summarised in section 2.5.5 for bacteria and in section 2.5.6 for phages.

2.3.3 Modelling phage growth in spatially unstructured liquid cultures

We developed a model of phage growth that takes several physiological processes into account: bacterial growth during the experiment, bacterial mortality due to

phage infection, phage mortality due to bacterial immunity. Lastly, growing phage populations require an active bacterial metabolism, their burst size β and latent period λ depend heavily on the actual bacterial growth rate (see Table 2.2).

The main processes in our model system can be defined by the following set of reactions,

$$B_\mathrm{s} + Y\,N \quad \xrightarrow{\alpha} \quad 2\,B_\mathrm{s}\ , \tag{2.2a}$$

$$B_\mathrm{r} + Y\,N \quad \xrightarrow{\alpha} \quad 2\,B_\mathrm{r}\ , \tag{2.2b}$$

$$B_\mathrm{s} + P \quad \xrightarrow{A} \quad \left(B_\mathrm{s}P\right) \xrightarrow{1/\lambda} \beta\,P\ , \tag{2.2c}$$

$$B_\mathrm{r} + P \quad \xrightarrow{A} \quad \left(B_\mathrm{r}P\right) \begin{cases} \xrightarrow{\text{fast}} & B_\mathrm{r}\ , \\ \overset{\ll 1/\lambda}{\dashrightarrow} & \beta\,P\ . \end{cases} \tag{2.2d}$$

Susceptible (B_s) and resistant (B_r) cells grow at a rate α, (2.2a) and (2.2b), by using an amount Y of the nutrients with concentration N. Phage infection involves first adsorption to host cells, (2.2c) and (2.2d), with an absorption term A specified below. Infected susceptible bacteria produce on average β phage with a rate inversely proportional to the average latency λ. In contrast, resistant bacteria either survive by restricting phage DNA via their CRISPR/Cas immune system or at some small rate succumb to the phage infection ($\ll 1/\lambda$). When multiplicity of infection (MOI) is large, however, even resistant cells are susceptible to lysis resulting in the release of phage progeny (Westra *et al.*, 2015; Chabas *et al.*, 2016).

In our system, bacteria eventually deplete the available nutrients N resulting in the cessation of growth. This decline in bacterial growth influences phage growth: latency increases and burst size decreases, such that phage reproduction declines dramatically (see Table 3). The critical time point at which cells transition from exponential growth to stationary phase is defined as,

$$T_\mathrm{depl} \approx \frac{1}{\alpha} \log\left(\frac{B^\mathrm{final}}{B^\mathrm{initial}}\right)\ . \tag{2.3}$$

Here, B^initial and B^final are the initial and final bacterial densities, respectively. In

the initial exponential growth phase, our estimates for growth parameters are $\alpha = 0.63\,h^{-1}$, $\beta = 85.6\,\mathrm{phages/cell}$ and $\lambda = 0.60\,h$, for bacteria and phages, respectively. Even though in reality the transition between exponential growth and stationary phase is smooth, in our model we use a simplified approximation that after time T_{depl}, bacterial growth rate is set to zero ($\alpha = 0$) and phage growth is reduced to $\beta_{\mathrm{depl}} = 3.0\,\mathrm{phages/cell}$ and $\lambda_{\mathrm{depl}} = 1.69\,h$. Although it is a simplified representation of bacterial growth, it still fits well the observed growth dynamics (see Fig. **??**) and allows us to analytically solve the system.

Reactions (2.2) can be recast into dynamical equations for averaged quantities, using densities B_{s}, B_{s} and P for the populations of bacteria and phages, respectively,

$$\partial_t B_{\mathrm{s}} = \alpha B_{\mathrm{s}} - A\big[B_{\mathrm{s}}, P|B_j\big]\ , \tag{2.4a}$$

$$\partial_t B_{\mathrm{r}} = \alpha B_{\mathrm{r}}\ , \tag{2.4b}$$

$$\partial_t P = \beta\, A\big[B_{\mathrm{s}}, P|B_j\big] - A\big[B_{\mathrm{s}}, P|B_j\big] - A\big[B_{\mathrm{r}}, P|B_j\big]\ , \tag{2.4c}$$

which is an approximation for very fast burst, $\lambda \approx 0\,h$. The probability of resistant cells failing to successfully mount an immune defence has a negligible contribution to the overall dynamics of the system and thus we ignore this term. A treatment of all processes in the set of reactions (2.2) is presented in Appendix 2.6.3. Adsorption of phages, given by the term $A\big[B_i, P|B_j\big]$, can be influenced by the whole distribution of populations within the culture. In liquid medium, a common assumption is that this term is proportional to the concentrations of both the phages and cells (Weitz, 2016),

$$A\big[B_i, P|B_j\big] = \delta B_i P\ , \tag{2.5}$$

with an adsorption constant δ. This expression assumes constant mixing of the population and relatively short contact times between phages and bacteria. In general, this system of equations is akin to Lotka-Volterra dynamics, which has been analysed in great detail, eg. (Hofbauer and Sigmund, 1998; Nowak, 2006).

We rewrite the set of equations in (2.4) as the total bacterial density $B = B_{\mathrm{s}} + B_{\mathrm{r}}$,

the fraction of susceptibles $S = B_{\mathrm{s}}/\big(B_{\mathrm{s}} + B_{\mathrm{r}}\big)$ and the phage density P, using the adsorption model from (2.5),

$$\partial_t B = \big(\alpha - S\delta P\big)B \,, \tag{2.6a}$$

$$\partial_t S = -S\big(1-S\big)\delta P \,, \tag{2.6b}$$

$$\partial_t P = \delta\big(S\beta - 1\big)BP \,. \tag{2.6c}$$

These equations reveal a time scale separation between the growth of the phage population and a significant change in proportion of susceptible individuals (S) in the population. The phage population undergoes explosive (double-exponential) growth before it affects composition of the bacterial population. In appendix 2.6.3.1 we show how simple phage growth implies that this explosive growth occurs (in almost all cases) before nutrients are depleted. Thus, as a first approximation, if the coefficient $\delta\big(S\beta - 1\big)B$ in (2.6c) is positive, we can assume that phages not only grow, but grow to large enough numbers to wipe the bacterial population. As the herd immunity threshold is related to the fraction of susceptibles via $H = 1 - S_c$, we combine these expressions to obtain the herd immunity threshold as

$$H = \frac{\beta - 1}{\beta} \,, \tag{2.7}$$

which shows very good agreement with the actual threshold between surviving and wiped out populations observed in experiments, see Fig. 2.1. In appendix 2.6.3.2 we expand the analysis to finite burst times $\lambda > 0$, to obtain the correction $\beta S_c - 1 - \lambda\alpha = 0$ for the critical condition. Thus, the herd immunity threshold extends as well to

$$H = \frac{\beta - 1 - \lambda\alpha}{\beta} \,. \tag{2.8}$$

The natural interpretation of this extension is that slower phage burst and faster bacterial growth lower the herd immunity threshold, compared to the prediction based on phage burst size only.

In section 2.3.1 we reported that phage growth parameters β and λ are strongly influenced by bacterial growth rate α. Thus, we also expect the herd immunity

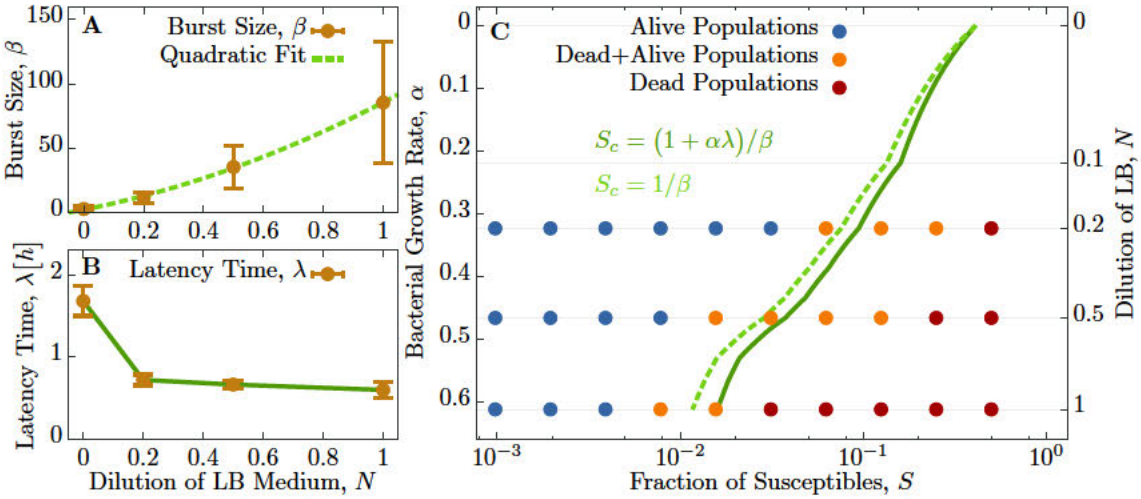

Figure 2.3: **Herd immunity threshold in liquid culture depends on bacterial growth.** (A) Measured phage burst size β changes with nutrient concentrations. A numerical fit quadratic in N seems to describe the observed values of β best (light green curve). (B) Latency times λ increase sharply at low nutrient concentrations while staying almost constant most of the range of nutrient concentrations. Values for both, β and λ are listed in Table 2.3. (C) The outcome of phage infection on bacterial populations depends on the fraction S of susceptible bacteria, but also on bacterial growth rate α tuned by nutrient concentration. Each coloured dot (blue, orange, red) represents the outcome of 18 measurements done in 3 independent batches. The herd immunity threshold $H = 1 - S_c$ (indicated by both green lines) predicts the crossover between dead and alive bacterial populations to a very good extent. The dashed light green line uses the prediction (2.7) and the quadratic fit shown in (A), which is transformed from N to α using measurements of bacterial growth presented in Table 2.2 and Fig. 2.5. The dark green line also includes the effects of finite latency times with H given by (2.8). Again, we used the transformation for the quadratic fit $\beta(N)$ and transform it numerically to $\beta(\alpha)$, together with another quadratic fit of $(\beta/\lambda)(N)$. Both $\beta(\alpha)$ and $(\beta/\lambda)(\alpha)$ are combined to $S_c = \big(\beta(\alpha)\big)^{-1} + \alpha\big((\beta/\lambda)(\alpha)\big)^{-1}$ to predict the dark green line.

	Estimate	*Units*	*Comment*
D	$1.17\ (\pm 0.26) \cdot 10^{-2}$	mm^2/h	See Section 2.5.7
α	0.63	h^{-1}	During exponential growth
$B_{\mathrm{s}}^{\mathrm{final}}$	$4.64\ (\pm 0.80) \cdot 10^{9}$	cfu/ml	In liquid overnight culture
$B_{\mathrm{r}}^{\mathrm{final}}$	$4.63\ (\pm 0.87) \cdot 10^{9}$	cfu/ml	In liquid overnight culture
$B^{\mathrm{final}}/B^{\mathrm{initial}}$	250		See Figure 2.5
T_{depl}	9.6	h	
$\delta^\star$	$2.91\ (\pm 0.08) \cdot 10^{-2}$	$\mathrm{cells/phage}\, h$	Estimate from (2.13) for spatial cultures

Table 2.1: **Model parameters.** All values above horizontal line are estimates from independent experiments, the adsorption constant $\delta^\star$ is obtained as fit using our model and all other parameters. Measurements for growth of bacteria and phages are listed separately in Tables 2.3.

threshold H should change significantly with varying α, because all parameters in (2.8) change, $H(\alpha) = \big(\beta(\alpha) - 1 - \lambda(\alpha)\alpha\big)/\beta(\alpha)$. Indeed, adjusting the the available resources by dilution of the LB medium, which determines the bacterial growth rate (see Fig. 2.5), shifts the herd immunity threshold (see Fig. 2.3).

All our model predictions assume a simplified scenario of bacterial growth dynamics. We assume that the growth rate is constant until bacteria enter the stationary phase at time T_{depl}, when the growth rate drops to zero. Although in reality this transition from exponential growth to stationary phase is a smooth (Fig. 2.5B), our simplification, which allows for much easier model analysis fits the observed dynamics reasonably well (see the green line in Fig. 2.5A).

2.3.4 Modelling phage growth in spatially structured surface populations

The dynamics of phage spread differ between growth in unstructured (e.g., liquid) and structured (e.g., plates) populations. In structured populations growth is a radial expansion of phages defined by the plaque radius r and the velocity v, for which several authors have previously derived predictions (Kaplan *et al.*, 1981; Yin and McCaskill, 1992; You and Yin, 1999; Fort and Méndez, 2002a; Ortega-Cejas *et al.*, 2004; Abedon and Culler, 2007; Mitarai *et al.*, 2016).

Host cell densities have a spatial dimension in addition to their time dependence, $B_i = B_i(\vec{x}; t)$; the subscript i indicates either susceptible (B_s) or resistant (B_r) hosts. However, the model assumes that only phages disperse and bacteria are immobile as the rate of bacterial diffusion does not influence the expanding plaque on timescales relevant in the experiment. Heterogeneity in the spatial distribution of bacteria is only generated by phage growth.

The size of the bacterial neighbourhood $\hat{B}$ that phages are able to explore is only slightly determined by the actual density B, and can be assumed constant for most of the experiment, $\hat{B}(B) \approx const$. Consequently, the adsorption term can be written in the following way,

$$A\big[B_i, P|B_j\big] = \delta^\star \frac{B_i}{\sum_j B_j} P \ , \tag{2.9}$$

which only depends on the *relative* frequencies of bacterial strains. The adsorption constant $\delta^\star$ is both the rate of adsorption and inter-host transit time as determined by the diffusion constant D. Thus, one can expect the formal dependence $\delta^\star = \delta^\star\big(D, \hat{B}(B)\big)$. For our particular experimental setup, however, $\delta^\star$ can be assumed constant. Writing the equations for B, S, and P, using the adsorption model in (2.9), yields,

$$\partial_t B = \alpha B - \delta^\star S P \ , \tag{2.10a}$$

$$\partial_t S = -\delta^\star S(1-S)P/B \ , \tag{2.10b}$$

$$\partial_t P = D\nabla^2 P + G\big[P, S\big] \ . \tag{2.10c}$$

where the dynamics of P is modified to account for the spatial diffusion with the additional term $D\nabla^2 P$. For simplicity, we consider only expansion in a single dimension ($\nabla^2 \equiv \partial_x^2$), which has been found to coincide well with the dynamics of plaque growth (Yin and McCaskill, 1992). The growth term for phages is then defined as,

$$G\big[P, S\big] = \delta^\star\big(S\beta - 1 - \lambda\alpha\big)P \ , \tag{2.11}$$

where we also consider the correction $\lambda\alpha$ obtained from the analysis in liquid

culture (see Appendix 2.6.3.2). Equations similar to (2.10c) have been previously analysed (Murray, 2002; van Saarloos, 2003; Fisher, 1937; Kolmogorov *et al.*, 1937). They admit a traveling wave solution – here, this corresponds to phages sweeping over uninfected bacterial lawn. In general, the asymptotic expansion speed for the traveling wave solutions is given by the following expression,

$$\begin{aligned} v &= 2\sqrt{D(\partial_P G)\big[0,S\big]} \\ &= 2\sqrt{D\delta^\star}\sqrt{S\beta - 1 - \lambda\alpha}\,. \end{aligned} \tag{2.12}$$

Only the linearised growth rate of phages at very low densities is relevant for the expansion speed, $\partial_P G\big[P=0,S\big]$. Thus, the fraction of susceptible individuals S should be unchanged from its initial value S_0. It should be noted, that only for $S_0\beta > 1+\lambda\alpha$ Eqn. (2.12) remains valid, otherwise we have $v=0$. Such a scenario when the expansion wave stops occurs when nutrients are depleted and phage growth parameters change to a low $\beta_{\mathrm{depl}} \sim 3$ and high $\lambda_{\mathrm{depl}} \sim 1.5h$ (so the fraction of resistant individuals becomes greater than the herd immunity threshold).

The expression for the expansion speed also shows the need for the spatial adsorption model in (2.9), in contrast to the liquid case (2.5). If adsorption would directly depend on the bacterial density B, the additional linear dependence on B in (2.11) would lead to an exponentially increasing speed during the experiment. This is in clear contradiction to experimental observations.

The density of phages behind the expanding front is large and as previously noted at large MOIs the CRISPR/Cas system fails to provide effective immunity (see section 2.5.4 and appendix 2.6.3.4). However, in comparison to an unstructured environment (e.g., liquid) the structured environment effectively limits transit of phage from within a plaque to expanding front: The combined effect of growth and diffusion usually generates a much faster expansion of phages during plaque formation, than diffusion alone. Only when nutrients are depleted, pure diffusion processes can explain the slow decrease in speed observed in experiments (see Fig. 2.7A). Our model assumes a sharp drop to $v=0$ at T_{depl} for small S.

In order to derive an expression for the plaque radius r, we integrate the

expansion speed (2.12) over time, $r = \int_0^t dt' v(t')$. Employing the simplification that only two values of phage growth are necessary to describe the dynamics – before T_{depl} phages grow normally with β and λ, after T_{depl} phage growth changes to β_{depl} and λ_{depl} (for the exact values see Table 2.3) – we can evaluate the integral for the radius directly, arriving at,

$$r = \begin{cases} 2t\sqrt{D\delta^\star}\sqrt{S\beta - 1 - \lambda\alpha}\,, & 0 < t < T_{\mathrm{depl}}\,, \\ 2\sqrt{D\delta^\star}\Big(T_{\mathrm{depl}}\sqrt{S\beta - 1 - \lambda\alpha} + \big(t - T_{\mathrm{depl}}\big)\sqrt{S\beta_{\mathrm{depl}} - 1}\Big)\,, & T_{\mathrm{depl}} < t\,. \end{cases} \tag{2.13}$$

Note that this expression remains valid only when the fraction of resistant individuals in the population is below the actual herd immunity threshold (Eqn. 2.14), otherwise the plaques cannot spread.

Using this expression we estimated the adsorption constant $\delta^\star$ from the growth experiments as it difficult in practice to easily measure. The green line in Fig. 2.2B is our best fit, yielding the value $\delta^\star = 2.91(\pm 0.08) \cdot 10^{-2}\,\mathrm{bacteria/phage}\,h$ for the adsorption constant.

In addition to using the plaque radius to understand population composition we can define the threshold at which the expanding plaque halts. Namely, the herd immunity threshold is reached when the last term in Eqn. (2.13) becomes negative,

$$H = \frac{\beta - 1 - \lambda\alpha}{\beta}\,. \tag{2.14}$$

It should be noted that the herd immunity threshold is independent of the additional parameters of the spatial case, the diffusion constant D, and the adsorption constant $\delta^\star$. We expect them to only generate additional subtle corrections.

Predictions of our model show a discrepancy from experimental results on plates. We independently estimated $\beta_{\mathrm{depl}} = 3.0$, which results in $H_{\mathrm{depl}} = \big(\beta_{\mathrm{depl}} - 1\big)/\beta_{\mathrm{depl}} \approx 0.67$. Thus, all experiments with $S > 0.33$ should exhibit expanding plaques after nutrients are depleted. In the experimental setup plaques stop expanding in all mixtures of resistant to susceptible cells ($S \leq 0.9$), which would correspond to $\beta_{\mathrm{depl}} < 1.1$. This value is, however, still within experimental accuracy of our estimates of β_{depl}.

Our results for spatial culture allows us to speculate on a general epidemiological question: If an infection is not stopped by herd immunity in a partially resistant population, by how much is its spread slowed down? By generalising (2.12) we can postulate a relative expansion speed, compared to a fully susceptible population,

$$v_{\mathrm{rel}} = \sqrt{\frac{R_0 S - 1}{R_0 - 1}} \,. \tag{2.15}$$

This expression, (2.15), is devoid of any (explicit) environmental conditions, which are not already contained in R_0. Thus, it could apply to any pathogen-host system. Ultimately, the only dependence of the relative speed of spreading in structured populations is on the growth properties of the pathogen R_0 and the resistant fraction of the population S.

2.4 Discussion

This report is the first to show that herd immunity may arise in phage-bacterial communities. The extent to which herd immunity occurs strongly depends on bacterial growth rates and the spatial organisation of the habitat they are growing in. As our results show, the herd immunity threshold H, (2.7) and (2.14), depends on phage growth via burst size β and latency time λ, but also on bacterial growth rate α. We also show that when populations are spatially structured, plaque expansion is significantly reduced even if the resistant fraction is far below the herd immunity threshold. We quantified these spatial effects by deriving expressions for expansion speed (2.12) and final plaque radius (2.13).

Our model has one free parameter, which was the adsorption constant $\delta^\star$ of phages. We used the measured plaque radius to fit this parameter, which could correctly reproduce the functional dependence on the fraction of susceptible individuals S. We expect that the absorption constant is influenced by the diffusion constant, and thus the combination of $D\delta^\star$ in equations (2.12) and (2.13) can be a seen as a single measure for all processes for the phage outside bacterial cells, also including the effects of the contact network between phage and bacteria.

Similarly, all processes within a single cell could be characterised by the growth parameters β, λ, and α. This allows us to group both internal and external processes of the phage spread, each with a single compound parameter. Consequently, also relative speeds (as measured with respect to other population compositions S and the same experimental conditions) only depend on these internal parameters as single combined parameter R_0 (2.15). This relative observables do not depend on the inferred parameter, and one might speculate about their importance and application in epidemiology, independent of a particular pathogen-host system.

Although our experimental system explores bacterial herd immunity under laboratory conditions, these environments may represent the extremes bacteria encounter in the wild, both in terms of growth rates and of spatial organisation. Average growth rates of bacteria in the wild have been estimated as substantially slower than those under optimal laboratory conditions (median generation time 6.5 fold longer (Gibson *et al.*, 2016)). Bacterial populations in the wild are also often structured, as bacteria readily form colonies or biofilms (Hall-Stoodley *et al.*, 2004) and grow in highly structured environments such as soil (Fierer and Jackson, 2006), the surface of leaves, or the gastrointestinal tract of animals. Since both reduced growth rate and spatial structure favour higher degrees of herd immunity, we predict that herd immunity is not unlikely in natural bacterial populations.

The fact that herd immunity can readily occur in bacterial populations may have substantial consequences for eco-evolutionary dynamics in phage-bacterial communities. While in a general deterministic situation a beneficial allele that arises in a population is eventually fixed, an allele that provides herd immunity can reach only the frequency equal to the herd immunity threshold. In other words, once the resistant allele reaches the herd immunity threshold frequency, pathogen cannot spread in the population and the allele cannot further increase in frequency because the selection pressure ceases. As a consequence, herd immunity has a potential to generate and maintain polymorphism in immunity-conferring loci, as has been studied in genes coding for the major histocompatibility complex (MHC) (Wills and Green, 1995). Polymorphisms in CRISPR spacer contents have been demonstrated in various bacterial (Tyson and Banfield, 2008; Sun *et al.*, 2016;

Kuno *et al.*, 2014) and archaeal (Held *et al.*, 2010) populations and communities (Pride *et al.*, 2011; Zhang *et al.*, 2013; Andersson and Banfield, 2008). While these studies mostly explain the polymorphisms in spacer contents as a result of rapid simultaneous independent acquisitions of new spacers, we propose that these polymorphisms may also be attributed to herd immunity. As a consequence, populations with high levels of CRISPR spacer diversity targeting a single phage are more robust to a phage escaping the CRISPR immunity by a mutation, than populations with a single spacer variant (van Houte *et al.*, 2016).

Besides the eco-evolutionary consequences for natural bacterial populations, herd immunity may also occur during phage therapy of infected wounds. Chronic bacterial infections of wounds typically exhibit biofilm formation (Hall-Stoodley *et al.*, 2004), thus, acquired CRISPR-based herd immunity may have substantial impact on efficacy of the treatment. Our results on agar plates are relevant to this: We showed that phage spread is significantly impaired, even if the fraction of resistant bacteria is below the herd immunity threshold.

2.5 Materials and Methods

2.5.1 Spacer insertion

Oligonucleotides AAACTTCGGGAAGCACTTGTGGAAG and AAAACTTCCACAAGTGCTTCCCGAA were ordered from Sigma-Aldrich and inserted onto pCas9 plasmid (available on addgene.org, plasmid #42876) carrying a *Streptococcus pyogenes* truncated CRISPR type II system. For the detailed protocol see (Jiang *et al.*, 2013). The oligonucleotides were chosen so that the CRISPR system targets an overlap of phage T7 genes 4A and 4B. Therefore, the CRISPR system allows the gene 0.7 coding for a protein, which inhibits the RNA polymerase of the cell, to be expressed before the T7 DNA gets cleaved (García and Molineux, 1995). The subsequent growth of the cells is thus halted but the phage replication is inhibited.

2.5.2 Time-lapse plaque assays

Soft LB agar (0.7%) containing 25 $\mu g/ml$ chloramphenicol was melted and poured into glass test tubes (VWR art.no.: 212-0308) heated to $43°C$ in a heating block. After temperature equilibrated, 0.9ml of bacterial cultures consisting of resistant and susceptible cells (ratios 10% – 100% of susceptible cells, 10% increments) were diluted 1 in 10 and added to the tubes. Then, 100ul of bacteriophage stock diluted appropriately to get ˜10 plaques per dish was added to the solution. Tubes were vortexed thoroughly and poured onto LB agar plates containing 25 $\mu g/ml$ chloramphenicol and distributed evenly using circular motion. After the soft agar hardened, the plates were placed on scanners (Epson Perfection V600 Photo Scanner) and scanned regularly every 20 minutes for 48 hours. Increase of individual plaque areas from time-lapse image series were then analysed with image analysis software PerkinElmer Volocity v6.3.

2.5.3 Herd immunity in a liquid culture

Herd immunity in a liquid culture was tested in LB broth supplemented with 25 $\mu g/ml$ chloramphenicol in Nunclon flat bottom 96 well plate in Bio-Tek Synergy H1 Plate reader. Bacterial cultures were diluted 1 in 1000 and mixed in the following ratios of resistant to susceptible cells: 50:50, 75:25, 87.5:12.5, 93.75:6.25, 96.88:3.13, 98.44:1.56, 99.22:0.78, 99.61:0.39, 99.8:0.2, 99.9:0.1, 99.95:0.05, 100:0 %. Phage T7 was added with multiplicity of infection (MOI) 10^{-4} and the cultures were monitored at optical density 600nm for 18 hours post innoculation (hpi).

2.5.4 Efficiency of the CRISPR/Cas system

Efficiency of the engineered CRISPR/Cas system was tested using the following protocol: Overnight culture was diluted 1 in 10, cells were infected with the T7 phage and incubated for 15 minutes in $30°C$. Cells were spun down for 2 min in room temperature at 21130g. Supernatant was discarded and the cell pellet was

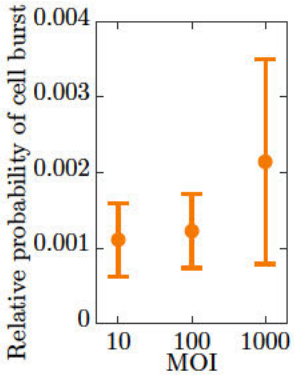

Figure 2.4: **Burst probability of resistant relative to susceptible cells.** If the number of phages increases, resistant cells burst more likely. Here, MOI is the initial ratio of phage population size to total bacterial population size. Experiments with MOI 10 and 1000 were conducted in 3 repeats with 4 replicates per repeat, experiments with MOI 100 in 4 repeats with 4 replicates per repeat.

resuspended in 950μl of Tris-HCl buffer containing 0.4% ascorbic acid pre-warmed to $43°C$ and incubated in this temperature for 3 minutes to deactivate free phage particles (Murata and Kitagawa, 1973). Cultures were serially diluted and plated using standard plaque assay protocol on a bacterial lawn of susceptible cells to detect bursting infected cells.

2.5.5 Estimating bacterial growth

2.5.5.1 Bacterial growth on soft agar

Growth rate of susceptible bacteria in soft agar was measured by sampling from a petri dish with a soft agar overlay with bacteria prepared in the same way as the plaque assays except an absence of the phage. Sampling was performed in spatially randomized quadruplicates at the beginning of the experiment and subsequently after 2, 4, 6, 8, 10, 12, 14, 16, 24, 32, 40, and 48 hours using sterile glass Pasteur pipettes (Fisherbrand art.no.: FB50251). Samples were blown out from the Pasteur pipette using an Accu-jet pro pipettor into 1ml of M9 buffer pre-warmed to $43°C$, vortexed for 15 seconds and incubated for 10 minutes in $43°C$ with two more vortexing steps after 5 and 10 minutes of incubation. Samples were serially diluted and plated on LB agar plates containing 25 $\mu g/ml$ chloramphenicol.

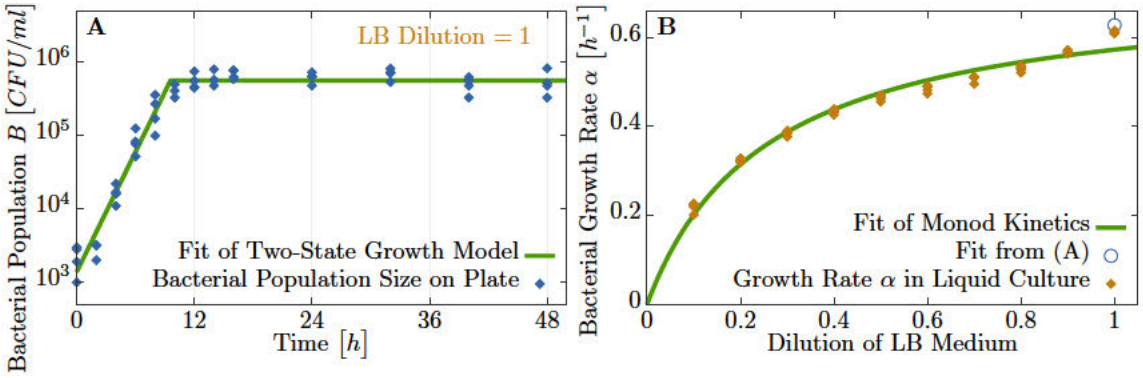

Figure 2.5: **Measuring bacterial growth without phage.** (A) Trajectory of population size on agar plates over time. For modelling, we assume two states of growth (green curve): first, the bacterial population grows exponential until the time T_{depl}, when nutrients are depleted. From this time on, growth rate is assumed to be zero and the population saturates at a maximal size B^{final}. Experimental observations fit this proposed growth curve to a very good extent. After all, half of all nutrients are used up in the last generation – with generation times of less than one hour, this the switch between growth and no-growth should be fast. (B) Growth rates of bacteria in diluted medium follow closely Monod's empirical law, given by expression (2.16). Fit parameters are found to be $\alpha_{\max} \approx 0.720\, h^{-1}$ and $K_c \approx 0.257$ (with the latter in dimensionless units as dilution of LB medium), see also Table 2.2.

	Estimate	*Units*
$\alpha_{\max}$	$0.720\ (\pm 0.011)$	$\left[h^{-1}\right]$
K_c	$0.257\ (\pm 0.012)$	Dilution N of LB $\left[0 \ldots 1\right]$

Table 2.2: **Estimated parameters for bacterial growth using Monod kinetics.** Undiluted LB medium ($N = 1$) is assumed to have $15\,mg/ml$ nutrients ($10\,mg/ml$ Tryptone, $5\,mg/ml$ yeast extract).

How bacterial densities evolve over time, measured as CFU/ml, is shown in Figure 2.5A.

2.5.5.2 Nutrient dependent bacterial growth rate in liquid culture

Growth rate of susceptible bacteria was measured in Nunclon flat bottom 96 well plate in Bio-Tek Synergy H1 Plate reader. Over night cultures were diluted 1:200 in media consisting of LB broth mixed with 1X M9 salts in ratios 10:90, 20:80, 30:70, 40:60, 50:50, 60:40, 70:30, 80:20, 90:10 and 100:0 %. Optical density at 600nm was measured every 10 minutes and the maximal growth rate was determined as a maximal slope of a linear regression of a sliding window spanning 90 minutes.

The resulting growth rates for various nutrient concentrations agree to a very good extent to Monod's growth kinetics,

$$\alpha = \alpha_{\max} \frac{N}{K_c + N} \ . \tag{2.16}$$

Results for the two fitting parameters, $\alpha_{\max}$ and K_c, are listed in Table 2.2, while the whole dataset, including the fit, is displayed in Figure 2.5B.

2.5.6 Estimating phage growth

2.5.6.1 Phage burst sizes

Phage burst sizes in bacteria growing at different growth rates were measured by one-step phage growth experiments. The burst sizes were calculated as the ratio of average number of plaque before burst to average number of plaques after

Medium	Dilution N	Latent period $\lambda\ [min]$	Burst size β	Burst size/hour $\beta/\lambda\ [h^{-1}]$
LB 0	0.0	$101.1\ (\pm 10.9)$	$3.0\ (\pm 1.9)$	$1.8\ (\pm 1.1)$
LB 20	0.2	$43.4\ (\pm 3.9)$	$12.0\ (\pm 4.2)$	$16.6\ (\pm 6.0)$
LB 50	0.5	$40.0\ (\pm 3.0)$	$35.6\ (\pm 16.4)$	$53.4\ (\pm 24.9)$
LB 100	1.0	$36.1\ (\pm 6.1)$	$85.6\ (\pm 47.3)$	$142.1\ (\pm 82.1)$

Table 2.3: **Estimated parameters for phage growth.**

burst. Consecutive samplings before and after burst were used for the calculation if they were not significantly different from each other (two sided t-test, $P > 0.05$).

2.5.6.2 Phage latent periods

Phage latent periods were determined as being within the time interval between the first and the last significantly different consecutive samplings between those used for phage burst size calculations.

2.5.7 Phage diffusion in soft agar

M9 salts soft agar (0.5%) was supplemented with SYBR safe staining (final conc. 1%) and poured into glass cuvettes (VWR type 6040-OG) to fill $\sim 2\,cm$ of the cuvette height. After soft agar solidification, the same stained soft agar was supplemented with T7 phage particles to a final concentration $10^{11}\,\mathrm{pfu/ml}$ and poured on top of the agar without phages. The cuvettes were monitored in $30°C$ every hour for 40 hours at the SYBR safe emission spectrum peak wave length $524\,nm$ illuminated with the SYBR safe excitation spectrum peak wave length $509\,nm$. The diffusion constant was estimated as the best fit parameter for the spread of fluorescent phages through the soft agar over time, as detailed in the next few paragraphs.

First we estimated the luminosity (i.e. grayscale value) of fluorescence in the images, and corrected the profiles of luminosity L_i by subtracting the background value. This background value was estimated as linear fit at the end of the profile without phages, where only the gray value of the agar was measured. Moreover,

luminosity saturates at values above ~ 0.4 and does not have a simple linear dependence on fluorescence: diffusion would lead to a decrease behind the edge and increase after the edge, but images only show increasing profiles – the bulk density does not decay. Thus, any estimate should only take the part of the profile that is below the threshold value of 0.4 into account (see Fig. 2.6).

The diffusion constant D itself was estimated as the minimal value of the total squared deviation of the convoluted profile $L^{(t)}$ (at time t) with a heat kernel $K(D)$ compared to the profile $L^{(t+1)}$ at time $t+1$,

$$D = \left\langle \min_D \sum_i \left(\left(\sum_j \frac{e^{-(i-j)^2/4D}}{\sqrt{4\pi D}} L_j^{(t)} \right) - L_i^{(t+1)} \right)^2 \right\rangle \ . \tag{2.17}$$

Such a convolution with the heat kernel $K_{ij}(D) = (4\pi D)^{-1/2} \exp\bigl(-(i-j)^2/4D\bigr)$ assumes that the only change in the profile is due to diffusion for a time span of length 1. Thus, expression (2.17) estimates the diffusion constant in units of $\mathrm{pixel}^2/\mathrm{frame}$, where frame is the time difference between two images. Several estimates are averaged over different snapshots in the whole experiment that spans $40\,h$ in intervals of $1\,h$ each.

The final estimate in appropriate units is

$$D \approx 1.17\ (\pm 0.26) \cdot 10^{-2}\ \ mm^2/h\ , \tag{2.18}$$

which seems to agree with other measurements on phage diffusion in the order of magnitude (Stent and Wollman, 1952; Bayer and DeBlois, 1974; Briandet *et al.*, 2008).

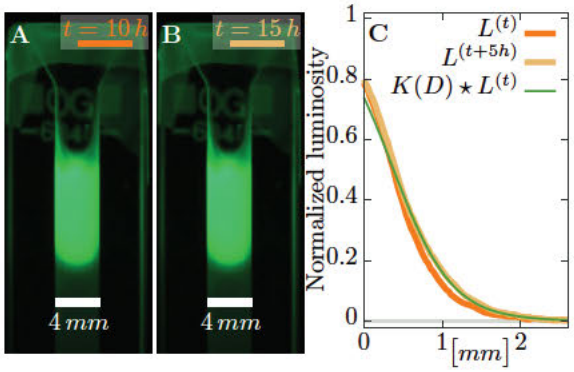

Figure 2.6: **Estimating diffusion constant of phages.** (A), (B) Phage are slowly expanding on agar which can be observed via their fluorescence. Pictures are taken $5\,h$ apart. (C) The diffusion constant D can be estimated as best-fit parameter in a *heat kernel* $K(D)$: $K(D)$ propagates the fluorescence profile $L^{(t)}$ at time t forward (via a convolution to "smear" out the signal) to the profile $L^{(t+\Delta t)}$ at the next measured time point. The difference between the expected change and the actual profile is quantified as total squared deviation, see Eq. (2.17), which we minimize to obtain D. Consequently, we can estimate the diffusion constant as $D \approx 1.17 \cdot 10^{-2}\, mm^2/h$. The green line uses this estimated parameter D and shows the change between the profile at $t = 10\,h$ (orange line, (A)) and the profile at $t = 15\,h$ (light brown line, (B)), assuming diffusive spread of phages. More details can be found in the supporting text.

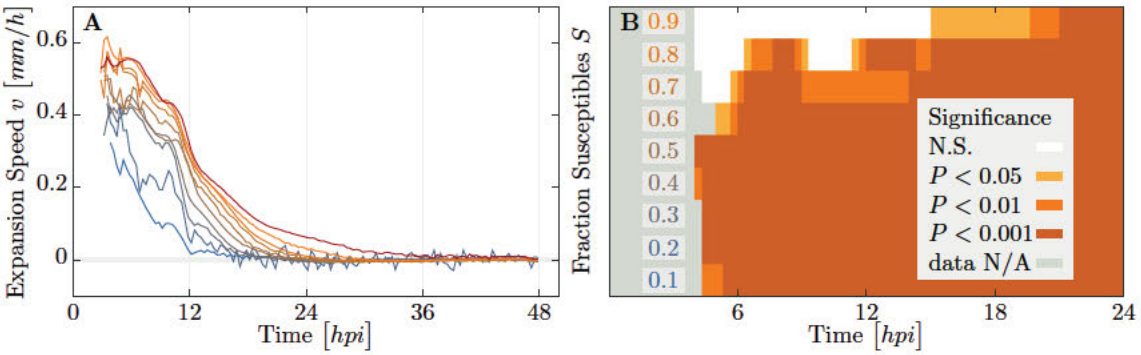

Figure 2.7: **Expansion speed of phages on bacterial plate culture.** (A) Expansion speed for all measured population compositions is initially high, before it drops after nutrients are depleted at around $10\,h$. (B) Plaque velocity significance. Comparing velocities of plaque spread with the 100% susceptible control. Linear regression of a sliding window spanning 4 hours of the radius sizes was calculated for all individual plaques and all compositions of the populations between t_0 and t_{24}. Slopes of the linear regressions for all compositions of the populations were compared using a two-sided heteroscedastic t-test with the 100% susceptible dataset.

$Variable\,/\,Parameter$	$Description$
B_s	Density of susceptible bacteria
B_r	Density of resistant bacteria
I_s	Density of infected susceptible bacteria
I_r	Density of infected resistant bacteria
B	Total density of bacteria
S	Fraction of resistant bacteria
$B^{initial}$	Initial density of bacteria
B^{final}	Final density of bacteria
N	Nutrient concentration
Y	Nutrient yield coefficient
T_{depl}	Time until nutrients are depleted
α	Growth rate of bacteria
P	Density of phage
A	Phage adsorption function
δ	Phage adsorption constant in liquid environment
$\delta^\star$	Phage adsorption constant in soft agar
β	Phage burst size
β_{depl}	Phage burst size on non-growing cells
λ	Phage latent period
λ_{depl}	Phage latent period on non-growing cells
ρ	Probability of recovery of resistant cells after phage infection
D	Phage diffusion constant in soft agar
G	Phage growth function on a soft agar plate
v	Velocity of phage epidemic spread
r	Plaque radius
H	See Box 1 for explanation
S_c	See Box 1 for explanation

Table 2.4: **Table of variables and parameters used in the model.**

2.6 Supplementary information

2.6.1 Table of variables and parameters used in the model

2.6.2 Significance of reduction in expansion speed

In Figure 2.7 we show the expansion speed for various population compositions. In a large majority of cases we actually find the reduction in expansion speed of the plaque is significantly different from the control experiment, which only contains susceptible bacteria.

2.6.3 Phage growth on growing bacteria

In the main text we stated that relevant processes for phages growing on bacteria are given by the set of reactions (2.2). In the following, we will analyse an extended version of our model, which takes all the processes into account. We try to justify our approximations and explain the reasoning behind leaving parts of the full model out. While reactions for single bacteria or phages are inherently stochastic in nature, we assume that the involved numbers are large enough such that the dynamics can be described with deterministic differential equations for the populations. Furthermore, reaction rates are identified with the inverse of the average time scale of the process. Thus, the full model is given by the coupled differential equations,

$$\partial_t B_\mathrm{s} = \alpha B_\mathrm{s} - \delta B_\mathrm{s} P \,, \tag{2.19a}$$

$$\partial_t B_\mathrm{r} = \alpha B_\mathrm{r} - \delta B_\mathrm{r} P + \rho I_\mathrm{r} \,, \tag{2.19b}$$

$$\partial_t I_\mathrm{s} = \delta B_\mathrm{s} P - (1/\lambda) I_\mathrm{s} \,, \tag{2.19c}$$

$$\partial_t I_\mathrm{r} = \delta B_\mathrm{r} P - (1/\lambda) I_\mathrm{r} - \rho I_\mathrm{r} \,, \tag{2.19d}$$

$$\partial_t P = (\beta/\lambda)\big(I_\mathrm{s} + I_\mathrm{r}\big) - \delta\big(B_\mathrm{s} + B_\mathrm{r} + I_\mathrm{s} + I_\mathrm{r}\big) P \,, \tag{2.19e}$$

$$\partial_t N = -(\alpha/Y)\big(B_\mathrm{s} + B_\mathrm{r}\big) \,. \tag{2.19f}$$

Both bacterial populations B_i grow with rate α and decay via adsorption of phages $A[B_i, P|B_j]$, an expression that is specified below. Infected populations I_i gain numbers by adsorption and decrease via bursting. Resistant bacteria also can recover from their infected state with a recovery rate ρ. Phages grow by bursting cells, and lose numbers by adsorption to the various bacterial populations. Moreover, explicit dynamics for nutrients is considered which is drained by each grown cell inversely proportional to the yield Y, which acts as conversion factor between nutrient concentration and cell numbers.

For many of the ensuing calculations it is important that bacteria grow exponentially in an initial phase. Phages growing on such exponentially multiplying bacteria can almost explode in number within a very short timespan. For such fast growth

it is important that nutrients are depleted at some point, limiting all populations to realistic sizes. The combination of these two effects, very fast growth and limited resources, is at the core of our argument that we can describe the outcome of all these dynamic processes with static conditions, as we did with when stating the herd immunity threshold.

For our ensuing analysis, we neglect the population of infected resistant bacteria I_r. Upon examining (2.19d) we find that most cells to leave their infected state by reducing phage DNA via CRISPR/Cas instead of bursting if $\rho \gg 1/\lambda$. If furthermore $\rho \gg \delta P$, which is true at least in the initial stages of the experiment, essentially all infected resistant bacteria immediately recover from a phage infection. Consequently, with both conditions, the resistant infected bacteria tend to vanish, $I_\mathrm{r} \to 0$, and their dynamics can be neglected.

2.6.3.1 Exponentially growing bacteria lead to double-exponential growth for phages

Having reduced the model by two equations by now, we can start to analyse the remaining ones in more detail. As in the main text, we transform the populations to the total bacterial density $B = B_\mathrm{s} + B_\mathrm{r}$, introduce the fraction of susceptible cells $S = B_\mathrm{s}/B$ and identify the total infected population with $I = I_\mathrm{s}$. Thus, we obtain

$$\partial_t B = (\alpha - \delta S P) B \,, \tag{2.20a}$$

$$\partial_t S = -S(1-S)\delta P \,, \tag{2.20b}$$

$$\partial_t I = \delta S B P - (1/\lambda) I \,, \tag{2.20c}$$

$$\partial_t P = (\beta/\lambda) I - \delta B P \,. \tag{2.20d}$$

Here, we assumed that the density of infected cells is much smaller than the actual bacterial concentration, $I \ll B$, such that we can ignore the drain in phage population that infect bacteria multiple times. The essential simplification is, however, assuming that phages burst immediately upon infection, $\lambda \approx 0$, which we also used in equations of the main text. As a consequence, phage dynamics

becomes $\partial_t P = (\beta S - 1)\delta B P$. We show that this is indeed the correct limiting behaviour more rigorously below.

If we assume that in initial stages of phage growth the number of phages is small, ie. $\delta P \ll \alpha \sim \mathcal{O}(1\,h^{-1})$, the dynamics of bacteria and the fraction of susceptibles simplify to $\partial_t B = \alpha B$ and $\partial_t S = 0$. Note that this term δP also occurs in the linear phage dynamics, but it is not considered a "coefficient" in this instance. Rather, we need to view δB as a coefficient, which is likely much larger initially, and we have to keep terms of order δP. This set of simplified equations can be solved in closed form,

$$S(t) = S_0\,, \tag{2.21a}$$

$$B(t) = B_0 \exp(\alpha t)\,, \tag{2.21b}$$

$$P(t) = P_0 \exp\big((S_0\beta - 1)\delta B_0(\exp(\alpha t) - 1)/\alpha\big)\,. \tag{2.21c}$$

The structure of phage dynamics is particularly important here – it exhibits a double-exponential dependence on time t, which is a very fast, almost explosive, growth. Such explosive growth is almost independent of the actual growth rate of phages, it only has to be positive. Thus, inspecting the exponent in (2.21c) yields the condition

$$\beta S_0 > 1 \tag{2.22}$$

for phage growth to be positive, which we identify with the the condition for dead bacterial populations, as stated in the main text. The double exponential time-dependence is essentially at the heart of our arguing that a "static" condition like (2.22) allows us to determine the dynamic effects.

An important question in the context of these solutions is whether nutrients run out before this explosive growth of phages occurs. Hence, we compute the time T_δ defined as when phages reach a population of $P(T_\delta) = 1/\delta$ assuming phages grow as (2.21c) until then. and compare it to the depletion time $T_{\mathrm{depl}} = (1/\alpha)\log(B_\infty/B_0)$.

Inverting (2.21c) for time leads to

$$T_\delta = \frac{1}{\alpha} \log \left(1 + \frac{\alpha \log(1/\delta P_0)}{(\beta S_0 - 1)\delta B_0} \right) \tag{2.23}$$

When rearranging the inequality $T_{\mathrm{depl}} > T_\delta$ in terms of the fraction of susceptibles S_0, we obtain

$$\beta S_0 > 1 + \frac{\alpha \log(1/\delta P_0)}{\delta(B_\infty - B_0)} \, . \tag{2.24}$$

This expression is a condition for phages to grow explosively before nutrients are depleted. The final population density B_∞ is usually large enough that $\delta B_\infty \gg 1$, such that the correction given by the second term of (2.24) can be considered small. Thus, if phages grow ($\beta S_0 > 1$), they also grow explosively with a double-exponential time-dependence and reach a considerably large population size before bacteria stop multiplying (for almost all parameter values).

2.6.3.2 Extending analysis to finite burst times

The analysis above only treated the case $\lambda \to 0$. However, we reported that the latency time λ increases significantly when bacterial growth rate α declines, see Table 2.3. Consideration of a finite latency time basically entails dealing with an infected bacterial population I. There are several ways to achieve this. First, we could directly solve (2.20b) to obtain the convolution

$$I(t) = \delta \int_0^t ds \; e^{-s/\lambda} S(t-s) B(t-s) P(t-s) \; , \tag{2.25}$$

using the initial condition $I(0) = 0$. Subsequently, this expression can be inserted into (2.20d) to obtain the dynamics of phages as

$$\partial_t P(t) = \frac{\beta\delta}{\lambda} \left(\int_0^t ds \; e^{-s/\lambda} S(t-s) B(t-s) P(t-s) \right) - \delta B(t) P(t) \; . \tag{2.26}$$

Equation (2.26) is a time-delayed differential equation, where the time-delay (or latency time) is exponentially distributed with parameter $1/\lambda$. This exponential

distribution of burst times arises due to the direct coupling with averaged rates in (2.19), and is born out of mathematical necessity rather than biological accuracy. In general, such time-delayed differential equations are hard, if not impossible, to solve in closed form.

However, one could take a slightly different route by combining the two equations (2.20b) and (2.20d), instead of inserting the solution of I into the dynamics of P. To this end, note that we can rearrange (2.20b) to $\big(1 + \lambda\partial_t\big)I = \lambda\delta SBP$. Hence, we can use the differential operator $(1 + \lambda\partial_t)$ and apply it directly to (2.20d) to reduce the dependence on I in this equation at the cost of introducing higher order derivatives. In particular, we obtain

$$\lambda\partial_t^2 P + \big(1 + \lambda\delta B\big)\partial_t P + \delta B(\beta S - 1 - \lambda\alpha)P = 0 \,, \tag{2.27}$$

where we also inserted $\partial_t B \approx \alpha B$ in the last term, as we aim again for a solution at initial times where $\delta P \ll \alpha$. Using (2.27) the effects of the limit $\lambda \to 0$ are directly observable – no terms are undefined in this limit. In particular, we find that equation (2.27) and $\lambda = 0$ lead directly to the dynamics of phages we just analysed above with the solution (2.21c).

In principle, (2.27) is a hyperbolic reaction-diffusion-equation, which is know to occur upon transformation (or also approximation) of time-delayed differential equations (Fort and Méndez, 2002b). Equation (2.27) can be investigated further: For initial times we can use the solutions $B(t) = B_0 \exp(\alpha t)$ and $S(t) = S_0$. To proceed, we introduce the auxiliary variable

$$z(t) = -\delta B_0 \exp(\alpha t)/\alpha \,, \tag{2.28}$$

which is essentially a rescaled bacterial population (with negative sign), and assume $P(z)$ as a function of this new variable z. We need to transform the differential operators of time derivatives, and obtain $\partial_t = \frac{\partial z(t)}{\partial t}\partial_z = \alpha z\partial_z$ and $\partial_t^2 = (\alpha z\partial_z)(\alpha z\partial_z) = \alpha^2(z\partial_z + z^2\partial_z^2)$. Inserting these expressions in (2.27) and multiplying the whole equation with $(\alpha^2\lambda z)^{-1}$ yields an accessible dynamics for

phages,

$$0 = z\partial_z^2 P(z) + (b - z)\partial_z P(z) - aP(z) \ , \tag{2.29}$$

where the two extant constants depend on parameters as $a = 1 - (\beta S_0 - 1)/(\lambda\alpha)$ and $b = 1 + 1/(\lambda\alpha)$. Equation (2.29) is called "Kummers equation" with confluent hypergeometric functions ${}_1F_1$ as solutions (Abramowitz and Stegun, 1964, pg. 504),

$$P(z) = A\,{}_1F_1\big(a, b; z\big) + B\,z^{1-b}{}_1F_1\big(a - b + 1, 2 - b; z\big) \ . \tag{2.30}$$

As we only allow real-valued function as solutions, we can directly set $B = 0$ as z^{1-b} contains a term $(-1)^{-t/\lambda}$ that is not defined over real numbers. In general, hypergeometric functions are abbreviations for series expansions – the solution with ${}_1F_1$ expanded in its original variables is given by

$$P(t) = A\sum_{n=0}^{\infty} \frac{\big(1 - (\beta S_0 - 1)/\lambda\alpha\big)_n}{\big(1 + 1/\lambda\alpha\big)_n} \frac{\big(-\delta B_0/\alpha\big)^n}{n!} e^{n\alpha t} \ , \tag{2.31}$$

with a second initial condition determining A via $P(t = 0) = P_0$. The terms in the first fraction of (2.31) involve Pochhammer symbols (or rising factorials) defined as $(a)_n = a(a + 1)\cdots(a + n - 1)$, $(a)_0 = 1$. From (2.31) we also recover the (double-exponential) solution (2.21c) in the limit $\lambda \to 0$. Thus, we expect (2.31) to have a similar shape, but more skewed with $\lambda > 0$. The most important aspect of (2.31) is to compute the parameters where it switches from a decreasing to increasing function over time. A careful analysis reveals that at $a = 0$ the behaviour of the solution changes. Consequently, we find the condition for growing phage populations,

$$\beta S > 1 + \lambda\alpha \ , \tag{2.32}$$

which is a non-trivial extension including finite latency times λ.

While this result is suggestive that it also should hold in the limit $\alpha \to 0$, it might not necessarily be so. This specific limit is actually quite important for the time when nutrients are depleted in the experiments. However, at several instances in the calculations above we implied a positive $\alpha > 0$. The most important of these is the transformation to $z(t) = -\delta B(t)/\alpha$, which actually exhibits two problems:

dividing by α should not be allowed and $B(t)$ is essentially constant and cannot serve as a variable in a differential equation. We also neglected the second term in $\partial_t B = (\alpha - \delta SP)B$ throughout our calculation. For $\alpha = 0$ this second term is dominant in bacterial dynamics and would generate non-linear phage dynamics if inserted for $\partial_t B$ right before stating (2.27). However, as an educated guess, we expect that albeit the process will run *very* slow, and might not be measureable in experiments, the simple condition $\beta S_0 > 1$ could indicate phage expansion and bacterial decay.

2.6.3.3 Simulation to determine recovery rate

Throughout this appendix we assumed that resistant bacteria are completely immune to phage infection as their CRISPR/Cas system immediately kills adsorbed phages. However, experimental observation suggest that for fractions close to what we predicted as herd immunity threshold, *all* bacteria eventually die. Thus, in the following section we use numerical simulations to investigate the full set of equations (2.19), with a particular focus on the question why the whole bacterial population goes extinct. As it turns out, this requires using finite values for the recovery rate ρ (instead of the $\rho \to \infty$ approximation we introduced at the beginning of this section).

A major difficulty in analyzing (2.19) is finding appropriate parameter values. In particular, we need the adsorption constant δ, the recovery rate ρ and the yield coefficient Y. Undiluted LB medium is known to support a population of $5{\cdot}10^9\ \mathrm{cells}/ml$ (see Table 2.1). Thus one can easily estimate Y as the inverse of this number, when nutrients are measured in units of dilutions, which we already used throughout this publication (undiluted medium corresponds to $N = 1$). Parameter scans in simulations reveal that the actual value of the adsorption constant δ does usually not influence the actual outcome (dead or alive bacterial population), it only adjusts time scales. However, deviations in time scales are insignificant, even when δ is changed by orders of magnitude, $\delta \sim \mathcal{O}\big(10^{-6} \dots 10^{-8}\big)$. They are roughly an hour or less, which is small compared to the expected duration

of the experiment that lasts a few hours. For definiteness, we use the value of $\delta = 10^{-7}\ h^{-1}$ for our simulations. That the value of the adsorption constant has only a minor impact on phage growth on bacterial cultures, is also in line with previous findings (Mitarai *et al.*, 2016).

The most elusive parameter is the recovery rate ρ. A first indication of the value of ρ can be drawn from our experiments on bursting resistant cells, summarised in Fig. 2.4. As the probability for bursting resistant cells is 3 orders of magnitude smaller than for susceptible bacteria, we can use $1/\lambda \sim \mathcal{O}(1)$ to estimate $\rho \sim \mathcal{O}\big(10^3\big)$. However, our results also indicate that recovery via the CRISPR/Cas system heavily depends on MOI, implying that ρ depends on the actual densities of phages and bacteria. Nevertheless, as experimental determination of recovery is complicated, even more so determining a functional dependence on dynamically changing densities B and P, we assume that ρ is constant.

We ran parameter sweeps in simulations and compared the outcome – dead or alive bacterial populations – to the observed experimental results (see Fig. 2.1). The best agreement of simulations and experiments was reached with $\rho \sim \mathcal{O}\big(1\big)$. Lower values of ρ do not allow the resistant population to recover from phage infection, while for larger values of ρ, phages are drained from the culture very fast. Such a small value of ρ is most likely related to the recovery at very large MOI, when the densities involved in the dynamics are large, which dominate the overall observed dynamics. At this time phages repeatedly infect the same bacteria and their CRISPR/Cas immune system cannot deal with such an infection load (or only too slowly). Thus, we can argue that our final choice $\rho = 1.5\ h^{-1}$ is the recovery rate when the CRISPR/Cas system is heavily stressed, which is compareable to the actual burst rate $1/\lambda$ for phages.

In Fig. 2.8 we show three exemplary sets of trajectories for bacteria and phage. For a tiny fraction of susceptibles, $S = 10^{-3}$, which is well below the herd immunity threshold (see Fig. 2.1), phages do not thrive on the limited number of favourable hosts and decay fast after a slight increase initially. For intermediate fractions of susceptibles, $S = 0.04$, we observe more complex, non-monotonic trajectories of bacterial populations. For such values of S we also observe mixed outcomes

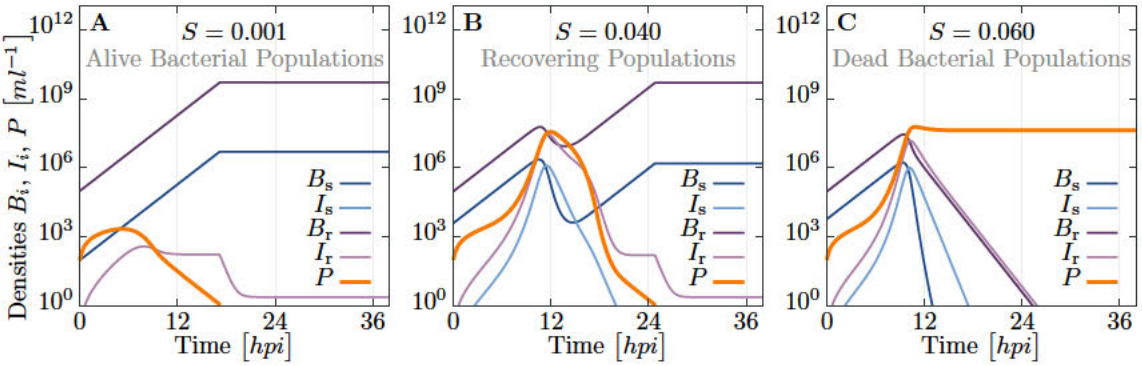

Figure 2.8: **Simulated trajectories for all populations in liquid culture for the extended model, including infected and recovering bacteria.** Trajectories are obtained by numerically integrating equations (2.19), using parameters listed in Table 2.1 and additionally $N = 1$, $Y = 2 \cdot 10^{-10}$ cells^{-1}, $\delta = 10^{-7}$ h^{-1} and $\rho = 1.5$ h^{-1}. (A) For population compositions with a large majority of resistant cells ($S = 10^{-3}$), phages get wiped out fast. (B) For intermediate S (close to parameters where we observe both, dead and alive, populations, see Fig. 2.1), the populations exhibit a complex, non-monotonic trajectory. After fast initial growth of phages, bacterial populations decay but ultimately can recover. (C) If the fraction of susceptibles is too large ($S = 0.06$), the whole bacterial population is infected and succumbs to the overwhelming phage infection. See supporting text for more detailed information.

in experiments, see Fig. 2.1. When S is increased further ($S = 0.06$), enough susceptible bacteria exists to produce enough phages and ultimately the whole bacterial population goes extinct.

The purpose of the extended model in this section was to justify the fact that phages can wipe out the whole bacterial population, which was not possible in the simplified model used in the main text. There, the resistant bacterial population was basically unaffected by phages and just acted as “sink” for phages. However, also in this extended model, we see a very similar behaviour in terms of the threshold phenomena reported in the main text and earlier in the appendix.

2.6.3.4 Infection load and efficiency of the CRISPR/Cas system

In sections 2.6.3.1 and 2.6.3.2 we showed that positive phage growth leads eventually to a very fast increase in the phage population, that occurs before nutrients are depleted (for almost all realistic parameters). This behaviour of the

dynamics was also observed in the extended simulation model presented in the last section. Moreover, whether the phage population reaches a size $P \sim 1/\delta$, which is after all arbitrary – it only determines if we can employ useful simplifications and approximations to model equations. However, simulation results presented in the last section 2.6.3.3 indicate that the bacterial population starts to decay soon after such a threshold $P \sim 1/\delta$ is exceeded.

In order to proceed, we assume that the phage population is large enough that it will not be degraded by the CRISPR/Cas immune system. The threat to immediate phage extinction is low at this point. The actual equations are hard to solve directly, hence we revert to simple balance equations, ignoring the dynamical component. Specifically, we compare the number of (present and eventually produced) phages to the number of infections needed to wipe out the whole population. To incorporate the effects of the bacterial immune system in resistant bacteria, we assume that they need $M > 1$ infections before they burst and produce only $\kappa\beta$ phages, which reduces the burst size by a (yet unspecified) factor $0 < \kappa < 1$. $\kappa = 1$ implies that resistant cells produce the same number of phages as susceptible cells, while $\kappa = 0$ indicates only cell death. Combining these considerations yields

$$\underbrace{1/\delta}_{\text{phages present}} + \underbrace{\beta S_0 B(T_\delta)}_{\text{phage production } B_\mathrm{s}} + \underbrace{\kappa\beta(1-S_0)B(T_\delta)}_{\text{phage production } B_\mathrm{r}} > \underbrace{S_0 B(T_\delta)}_{\text{infections } B_\mathrm{s}} + \underbrace{M(1-S_0)B(T_\delta)}_{\text{infections } B_\mathrm{r}}, \tag{2.33}$$

where the left side indicates the total number of phages, while the right side indicates the number of necessary infections to kill all bacteria. The number of bacteria $B(T_\delta)$ can be estimated by inserting the time T_δ from (2.24) into the exponential growth (2.21b). Subsequently, we can rearrange (2.33), obtaining a bound on M:

$$M < \frac{1/\delta B(T_\delta) + S_0((1-\kappa)\beta - 1) + \kappa\beta}{1 - S_0}\,. \tag{2.34}$$

The first term in the denominator $1/\delta B(T_\delta)$ is small for non-extremal parameters when compared to the other terms, which justifies our assumption that the actual value of δ is not crucial. This number M might allow some insight into the effectiveness of the CRISPR/Cas immune system. For a fraction of susceptibles

$S = 0.03$, which corresponds to the minimal value where we observe only dead bacterial populations in undiluted LB medium (see Figs. 2.1 and 2.3), we would obtain the relation $M \lesssim 3 + 86\kappa$. Thus, each resistant bacterial cell could degrade up to $\mathcal{O}\big(10^1 \dots 10^2\big)$ phages before their CRISPR/Cas system cannot cope with the infection load anymore.

2.6.3.5 Considerations for spatial growth on plates

So far, with equations (2.19), we analysed the extended model for population in unstructured liquid medium. In spatial cultures, we can argue similarly that the addition of infected populations that can recover will lead to the patterns we observe: Within the plaque, all bacteria (susceptible and resistant) die due to phage infection, but obviously bacteria survive in regions not reached by phages.

3 Pheromone mediated bacterial social immunity

3.1 Abstract

Social immunity mostly requires transmission of information describing the health status of the sick individual to healthy individuals. In this chapter, we explore the potential for pheromone mediated bacterial social immunity using both bioinformatic and experimental approaches in *Streptococcus thermophilus* and its phage 2972. We employ a bioinformatic analysis of potentially coding short open reading frames with a signalling signature, encoded within the CRISPR associated genes. Subsequently, we test one identified potentially signalling peptide and show that its addition to a phage-challenged cultures increases probability of survival of bacteria 2 fold. Although the results were only marginally significant, they indicate a framework for future exploration of pheromone mediated social immunity in bacteria, particularly for an investigation of potentially coding short open reading frames encoded within other coding sequences.

3.2 Introduction

Bacterial herd immunity is an effective and viable mechanism for defence against viral pathogens and may be relatively common in bacterial populations (see Chapter 2). The observation that resistant individuals reduce the transmission probability

of a pathogen from one susceptible host to another is in this case a byproduct of selection on the individual immune response. In addition to this 'side effect', the probability of transmission can also be reduced by other processes, such as social immunity, which cannot be explained solely by natural selection on the individual. Social immunity is defined as 'any collective and personal mechanism that has emerged and/or is maintained at least partly due to the anti parasite defence it provides to other group members' (Meunier, 2015). Thus, in a group living organism any behaviour that reduces the pathogen or parasite load on the group falls under this definition, even though it may not directly increase the fitness of the acting individual. This form of immunity occurs in many animals such as ants and great apes in the form of allogrooming, a behaviour in which one individual grooms another to remove ectoparasites, or through hygienic behaviours such as when ant workers remove diseased brood from the nest (Wilson *et al.*, 2003; de Roode and Lefèvre, 2012). For a review on social immunity in insects see Meunier (2015). In humans, three general social behaviours can be considered under this definition. First, a reduction in social interactions with other people with the intent of preventing transmission. Second, healthy individuals often avoid contact with sick individuals. Third, seeking medical care for treatment by a physician. In all cases, these behaviours while not necessarily increasing the fitness of the acting individual does always contribute to limiting the spread of the pathogen.

Often these social immunity behaviours are preceded by the transmission of information describing the health status of the sick individual (e.g., 'I am sick') to healthy individual(s), or by recognition of the symptoms by the acting individuals.

It is evident that social immunity has evolved many times in group living organisms, particularly in groups with high relatedness because low population diversity facilitates spread of pathogens (King and Lively, 2012). As bacteria often live in structured environments and produce clonal offspring, *i.e.*, live in groups with very high relatedness, it would be particularly beneficial for them to be able to react to a phage epidemic not only on an individual level but also as a population. As we have said above, this step would require some sort of communication and cooperation. Therefore, in order to start considering social immunity in bacteria,

one has to first take into account what could be the means of communication that would carry the information to increase the survival probability after a phage infection, for example to over-express genes involved in immunity.

In this chapter, we show that bacterial communication and cooperation is not a rare phenomenon and describe how this communication and cooperation is achieved in different concerted population-wide phenotypes. We first describe the roles and abundances of small functional peptides in general and then introduce a special group of these peptides, which are involved in pheromone signalling, *i.e.*, cell to cell communication in gram-positive bacteria. Subsequently, we present our research on the identification of a putative CRISPR/Cas immunity linked signalling peptide and its experimental verification.

3.2.1 Small functional peptides

Short open reading frames (sORFs), which code for small peptides, have historically been mostly disregarded, largely due to difficulties in detecting their products. Only recently, advances in bioinformatic and experimental methods have started to reveal their coding sequences and functions. sORFs been identified in all kingdoms of life, including humans, species of *Drosphila, Arabidopsis,* yeast (Andrews and Rothnagel, 2014), many bacteria (Hobbs *et al.*, 2011) and some archaea (Mackin, 2011). In Eukaryotes, sORFs encoding small peptides have been found in a variety of genomic locations: Upstream of coding sequences (CDS) in the the 5' untranslated regions (UTRs), in between CDS, and, interestingly, overlapping with CDS. To our best knowledge, in bacteria only intergenic sORFs have been identified so far but the evidence of overlapping antisense-encoded long ORFs (Merino *et al.*, 1994) suggests that also CDS overlapping sORFs are potentially possible. Small peptides vary greatly in terms of their function, which ranges from intracellular regulatory elements, protein-stabilising and structural units, to signalling molecules (Hobbs *et al.*, 2011; Andrews and Rothnagel, 2014). Since our aim is to investigate the potential of sORFs in social immunity, we now focus on a large group of small peptides involved in bacterial communication – bacterial

pheromones.

3.2.2 Pheromone signalling in bacteria

Passage of information from one individual to another in bacterial world is mediated by small molecules called pheromones in a phenomena called quorum sensing. Pheromones produced by bacteria usually accumulate in the environment with increasing cell density and trigger a signalling event when a threshold density ('quorum') has been reached. Although there is evidence that this signalling can also occur between members of different species (Miller and Bassler, 2001; Cook and Federle, 2014), in this chapter we will only consider intraspecific signalling. Also, not all responses are conditioned by population-wide reaction to a threshold density of a pheromone but some, such as for example conjugation, occur directly between neighbouring cells. Since our aim is to investigate potential of pheromone signalling in bacterial social immunity against phages, we also discuss these direct communications.

Pheromones have been shown to induce several phenotypes such as virulence (Rutherford and Bassler, 2012), competence development (Fontaine *et al.*, 2010; Håvarstein *et al.*, 1996), bacteriocin production (Eijsink *et al.*, 2002; Quadri, 2002), bioluminiscence (Miller and Bassler, 2001), biofilm formation (Jayaraman and Wood, 2008; Parsek and Greenberg, 2005), conjugation (Lyon and Novick, 2004; Grohmann *et al.*, 2003), sporulation (Steiner *et al.*, 2012; Perego *et al.*, 1996), or plant infection (Cha *et al.*, 1998).

The chemical nature of these small signalling molecules differs between gram-negative and gram-positive bacteria. While gram-negative bacteria usually communicate using small molecules such as N-acyl homoserine lactones, gram-positive bacteria mostly communicate using small peptides (Lyon and Muir, 2003). Because our experimental system consists of a gram-positive bacterial species, *Streptococcus thermophilus,* and its phage, we will focus strictly on small peptides and briefly discuss the main roles in signalling they mediate.

Currently four different groups of gram-positive bacterial pheromones have

been described, differing in their features and their receptors (Cook and Federle, 2014): (1) Members of RNPP, (2) Agr-type cyclic peptides, (3) Gly-Gly peptides, and (4) Rgg regulators and short hydrophobic peptides.

RNPP pheromones have been shown to be involved in conjugation and biofilm formation in *Enteroccocus faecalis*, virulence in *Bacillus anthracis*, and competence and sporulation in *Bacillus subtilis.* They are short oligopeptides which are processed (cleaved at certain sites) after translation, exported out of the cell, transported into the recipient cell by an oligopeptide permease and then bind to their cognate intracellular receptor protein. (Rocha-Estrada *et al.*, 2010).

The second group of pheromones of gram-positive bacteria are Agr-type cyclic peptides. These peptides are involved in virulence in *Staphylococcus aureus* and at least 15 other *Staphylococcus* species and in *E. faecalis.* Agr-type oligopeptides are also processed after translation but in a different way – while the N-terminal processing is again a simple proteolytic cleavage, the C-terminus is cleaved and circularised. This C-terminal ring is a hallmark of Agr-type peptides and plays a crucial role in detection of the signal, which also differs from the RNPP peptides. The Agr pheromones are sensed by a dedicated two-component signal transduction pathway. Thus, the pheromone binds to a histidine kinase on the surface of the recipient cell, which transmits the signal further via phosphorylation of a cytoplasmic response regulator (Lyon *et al.*, 2002; Steiner *et al.*, 2012).

Gly-gly peptides are known to regulate competence and production of bacteriocins in *B. subtilis* and some *Streptococci.* These peptides are characterised by a double-glycine (GG) motif in their conserved leader sequence, after which the peptide is cleaved and the residue is exported out of the cell. Similarly to Agr pheromones, Gly-gly peptides are also sensed via a two component transduction pathway (Cook and Federle, 2014; Håvarstein *et al.*, 1996).

The last group are Rgg pheromones, which have been shown to be involved in competence development and biofilm formation in many *Streptococci.* They are similar to RNPP pheromones in the fact that they are internalised and bind directly to their intracellular regulator. Processing of Rgg pheromones is, however,

more complicated and they are not only modified within the cell where they are produced, but also outside the cells in the extracellular environment by an additional yet unknown exported enzyme. Also, Rgg pathways are thought to be able to integrate both intercellular signalling and environmental stimuli into a single adaptive response (Fontaine *et al.*, 2010; Mashburn-Warren *et al.*, 2012).

Albeit the four pheromone types described above differ in many details, they share one crucial feature, which can be used as a clue for identification of other putative signalling peptides – they all have a leader sequence, which has a conserved molecular hallmark indicating a potential signalling molecule. All the groups have a N-terminal 'handle', which is recognized by a conserved protein exporting machinery of the cell, the translocase, and subsequently cleaved while the C-terminal part of the protein is being exported out of the cell (Manting and Driessen, 2000).

3.3 Results

3.3.1 *In silico* analysis

We analysed the CRISPR/Cas operon of *S. thermophilus* DGCC7710 for CDS overlapping sORFs, which resulted in 444 positive results, both on the sense and antisense strands. Then we analysed *in silico* translations of these sORFs for the signature of a signalling peptide, which resulted in 6 putative sORFs within the *cas9* CDS. Subsequently, we ran an analysis of the upstream regions of these potential signalling sORFs looking for putative promoters. This further narrowed down the list to a single sORF on the antisense strand whose upstream region contained a predicted -10 and -35 box (see Fig. 3.1 for the nucleotide sequence and annotations). We named this putative peptide Pcrap - potential CRISPR activating peptide. Its amino acid sequence is MVMISITSLLNSPMASQ–LRCKLATNHGNFCINLVSSKVFLKGIEDNS and the predicted proteolytic cleavage site is located between positions 17 and 18: ASQ–LR (indicated by a dash in the sequence, for full results of the test see Fig. 3.2 and Table 3.2).

ORF	Start:End	Translation Initiation Rate	Translation Coupling Factor	ΔG_{total}	ΔG	ΔG_{start}
cas9	0:3363	1.32	1	16.76	17.36	-1.19
pcraP	0:141	0.7	1	18.16	17.36	-1.19

Table 3.1: *In silico* analysis of translation of *cas9* and putative signalling peptide Pcrap using De Novo DNA Inc. Operon Calculator (Tian and Salis, 2015).

Measure	Position	Value	Cutoff	signal peptide?
max. C	18	0.138		
max. Y	18	0.302		
max. S	15	0.826		
mean S	1-17	0.651		
D	1-17	0.494	0.420	YES
Name=Pcrap	SP='YES' Cleavage site between pos. 17 and 18: ASQ-LR D=0.494 D-cutoff=0.420 Networks=SignalP-noTM			

Table 3.2: Results of SignalIP 4.1 analysis of Pcrap

The predicted promoter region of *pcraP* also contains a predicted regulatory region binding rpoD17 and/or rpoD15 transcription factors (TFs). The rpoD TFs (sometimes called sigma 70 TFs) are global TFs regulating diverse processes in the cell and provide a concerted expression of genes involved in many physiological processes such as, stress responses, sporulation, iron uptake (Paget and Helmann, 2003) and virulence (Miura *et al.*, 2015). Although sigma 70 factors show high homology among various bacterial species, they differ in their roles in different species and to our best knowledge, none have been experimentally investigated in *S. thermophilus.* Interestingly, an analysis of the promoter region upstream of *cas9* showed that this gene is regulated by the same TF rpoD17. This evidence suggests that expression of the CRISPR/Cas immune system, namely of *cas9,* is coordinated with expression of the putative signalling sORF.

The last step of our *in silico* analysis was to look for a ribosome binding site between the promoter sequence and the start codon and determination of the translation rate of the peptide. This analysis showed a comparable translation initiation rate and ribosome binding affinities to that of *cas9* (see Table 3.1 for the details).

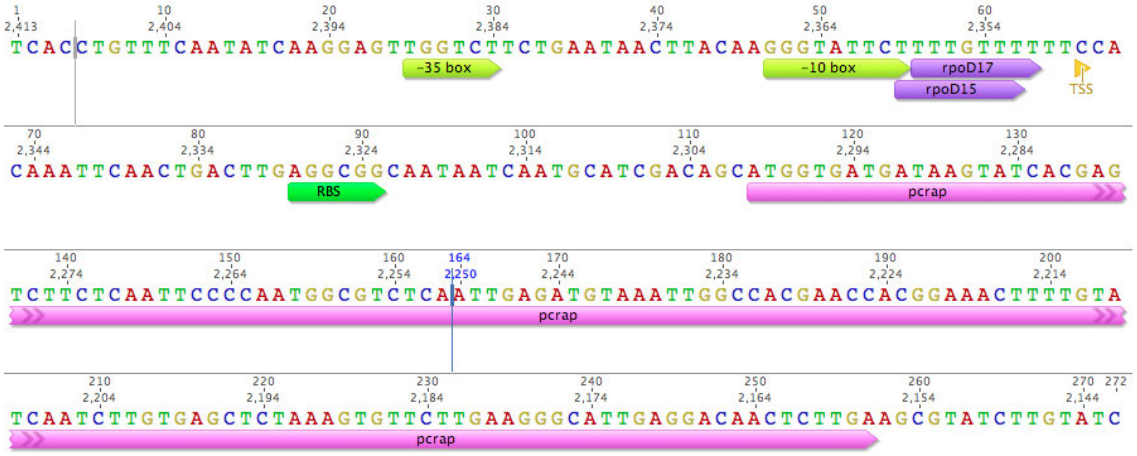

Figure 3.1: Annotations of the *pcrap* genomic region. Nucleotide sequence of *pcrap* (pink) and it its upstream region with annotated -10 and -35 box (yellow), rpoD15 and rpoD17 TF binding sites (purple), transcription start site (TSS, orange) and ribosome binding site (RBS, green).

3.3.2 Experimental verification

In order to evaluate whether the predicted signalling peptide Pcrap induces immune response in *S. thermophilus*, we ordered a synthetic version of the cleaved Pcrap and tested whether its addition to a culture increases survival of the bacteria when challenged by phage 2972. Our results show that the mean ratio of surviving colony forming units (CFUs) of the population with Pcrap supplementation vs. control was 2.1 (Fig. 3.3).

3.4 Materials and methods

3.4.1 Potential sORF identification

We analysed the CRISPR/Cas operon of *S. thermophilus* DGCC7710 using Geneious® 6.1.7 looking for all sORFs with length ranging between 10 and 70 codons on both sense and antisense strand.

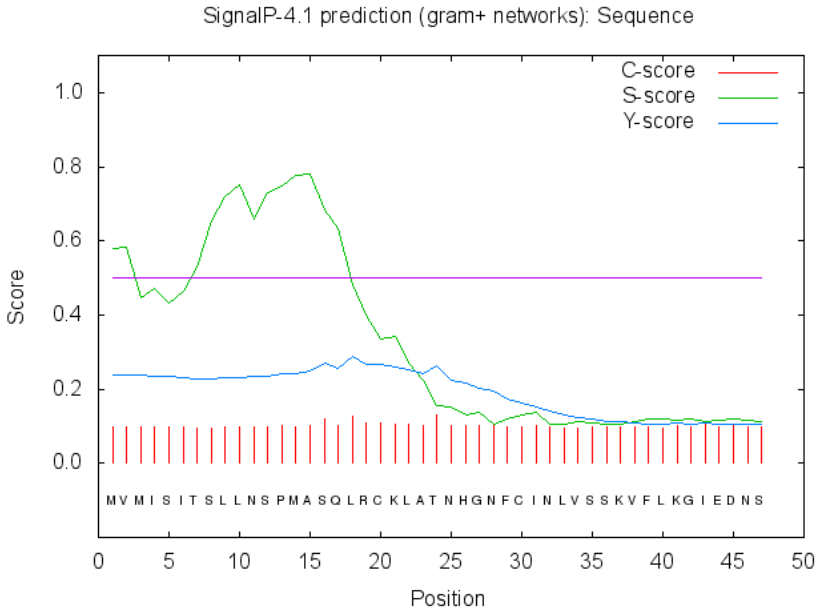

Figure 3.2: Results of *in silico* analysis of Pcrap amino acid sequence. The analysis was performed using SignalIP 4.1 (Petersen *et al.*, 2011). C-score (raw cleavage site score): The output from the CS networks, which are trained to distinguish signal peptide cleavage sites from everything else. S-score (signal peptide score): The output from the SP networks, which are trained to distinguish positions within signal peptides from positions in the mature part of the proteins and from proteins without signal peptides. Y-score (combined cleavage site score): A combination (geometric average) of the C-score and the slope of the S-score, resulting in a better cleavage site prediction than the raw C-score alone. This is due to the fact that multiple high-peaking C-scores can be found in one sequence, where only one is the true cleavage site. The Y-score distinguishes between C-score peaks by choosing the one where the slope of the S-score is steep (Petersen *et al.*, 2011)

.

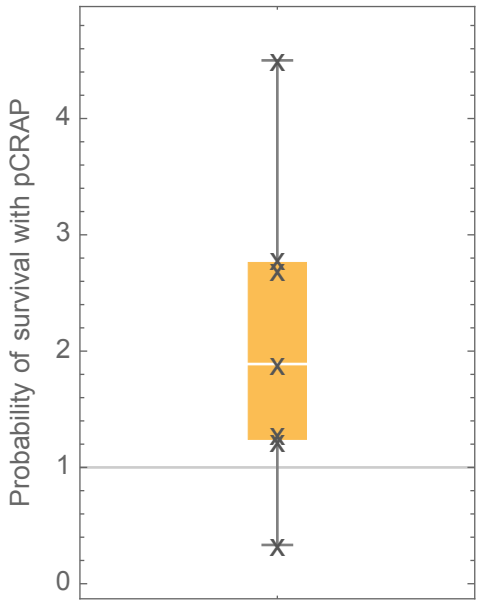

Figure 3.3: Results of Pcrap induction assays. Boxplot showing the probability of survival of the Pcrap induced cultures after exposition to phage relative to the non-induced control. Values of individual experiments are indicated by ”x” symbols. The mean of the ratios is statistically significant from 1 (p-value = 0.03827, t-statistic = 2.1362). For more details see Materials and Methods, sections 3.4.3 and 3.4.4.

.

3.4.2 Potential signalling sORF identification

We translated all sORFs found in the previous step *in silico* using Geneious® 6.1.7 and analysed them for a signature of a signalling peptide using SignalIP 4.1 (Petersen *et al.*, 2011). Subsequently we analysed their upstream regions (150bp) with SoftBerry BPROM (Solovyev and Salamov, 2011).

3.4.3 Pcrap induction assays

We inoculated overnight (OVN) cultures in M17 medium pre-warmed to 42°C 1:50 and let the cells grow in a shaking incubator at 42°C until an $OD_{600} \sim 0.25$. After the cells reached this population density, we added Pcrap to a final concentration of $10\mu M$ to the test tubes and distilled water of a corresponding volume to the control. We incubated the tubes at 42°C for additional 30 minutes and then added phage

2972 at a multiplicity of infection (MOI) $\sim$ 1 and 10mM CaCl into both test and control tubes. Then we incubated the tubes with bacteria and phages for additional 2 hours until the cultures cleared (complete lysis) and subsequently plated serial dilutions of the supernatant on M17 agar plates. We counted emerging colonies after two days of incubation at 42°C.

3.4.4 Pcrap induction statistics

We performed a statistical analysis of the difference in the number of CFUs in the Pcrap treated and control tubes. Every sample was normalised by the number of CFUs in the control tube and the difference was compared to 0 using a paired one-sided T-test. Null hypothesis was that Pcrap has no effect, alternative hypothesis that CRAP increases the probability of survival.

3.5 Discussion

Induction of immunity by the addition of our candidate signalling CRISPR/Cas activating peptide (Pcrap) increased survival probability of the treated bacteria 2.1 times, although this finding was only marginally significant. The rather weak effect of the peptide can be attributed to several factors: First, as we have described above in section 3.2.2, bacterial signalling pro-peptides are often not only cleaved at the site between the C-terminal handle and the N-terminal signalling peptide (which is a signature of signalling peptides) but also further processed. This further processing often involves additional cleavage of the signalling peptide at other sites (for example see processing cascade of a conjugation pheromone of *E. feacalis* in Table 3.3). Other peptides, like the Agr pheromones, are further modified to form a ring structure at the N-terminus by forming a lactone or thiolactone ring. Their modifications result in high variations in signalling efficiency in different *S. aureus* groups and often the modified peptides competitively suppress their functional analogs (Lyon *et al.*, 2002). Thus, if our candidate peptide requires further modifications, its non-processed form may only have a minor effect. Second,

some bacterial signalling pathways are predicted to be able to integrate not only information from the signal itself but also information from the environment (Camilli and Bassler, 2006). It is reasonable to expect that if social immunity occurs in bacterial populations, it has evolved to suppress phage spread rather in structured populations. Therefore, the effect of the Pcrap supplementation may be reduced in a well mixed liquid environment we used in our experiments.

MKKYKRLLLMAG**LVTLVFV**LSACGTAPVSESSTGIWDRYIV...		
↓	Signal peptidase II	} Membrane translocation
MKKYKRLLLMAG**L**VTLVFVLSA		
↓	Metalloprotease	
LVTLVFVLSA		
↓	Exopeptidase	
LVTLVFV		

Table 3.3: Processing of the *Enterococcus faecalis* conjugation peptide cCF10. Processing of the pro-peptide occurs via at least three separate cleavage events upstream of the amino acids indicated in red. Signal peptidase II cleaves the lipoprotein upstream of a cysteine residue. The peptide precursor is then cleaved during the transport process, likely by a metalloprotease. The pro-peptide is secreted into the extracellular environment where it is further cleaved by an exopeptidase, removing the terminal three amino acids to yield the cCF10 peptide pheromone which can be sensed by neighbouring cells. Modified from (Cook and Federle, 2014).

There is also a possibility that the increased survival is because the peptide is interfering or inactivating some of the phages rather than signalling to the other cells (Killmann *et al.*, 1995), and we did not conduct additional experiments to rule this option out. However, indirect evidence that bacterial signalling as a response to phage infection exists. First, the average plaque size of phage 2972 on a bacterial lawn of *S. thermophilus* is substantially smaller (*cca.* 10 fold, data not shown) than plaque sizes of other comparable phage-bacterial systems, for example the *E. coli*–phage T7 system we studied in chapter one. As we have shown in Chapter 2, the velocity of spread (and subsequently the plaque size) is determined by phage burst size, its diffusion constant and adsorption rate. Phage capsid diameter and burst size have been shown to be comparable with coliphage T7. Burst size of the wild type phage 2972 has been estimated as 190 ± 33 (Deveau *et al.*, 2008) which is very close to an estimate of maximal burst size of T7 on cells growing in 37ºC,

which is 179 ± 19 (Nguyen and Kang, 2014). The capsid size, which is likely the main determinant of phage diffusion has been estimated as 55nm both in phage 2972 and T7 (Lévesque *et al.*, 2005; Cerritelli *et al.*, 1997). Although we could not find measurements of adsorption rate *per se* of the phage 2972, adsorption tests have been carried out showing that 95.9% ± 1.7% of the phage particles adsorb to cells within 10 minutes after inoculation with MOI ~ 10^{-3} at 42ºC (Duplessis *et al.*, 2005). This suggests that the adsorption rate of phage 2972 is even higher than of T7, where only 26.9% of the phages adsorb within 7 minutes after inoculation with similar MOI (Bleackley *et al.*, 2009).

Although the small plaque sizes could be possibly explained also by production of an extracellular substance, which limits spread or adsorption of the phages, another observation indicating existence of bacterial signalling in response to phage infection exists. It has been shown by Levin *et al.* (2013) that the number of surviving *S. thermophilus* bacteria after phage 2972 inoculation is higher than predicted by a model, which takes into account all known processes of phage spreading in a bacterial population. Only after allowing for some sort of resistance induction by a pheromone in their model, its predictions showed a good agreement with the observed results.

3.5.1 Future directions

The phenomenon of bacterial pheromone signalling in *S. thermophilus* and phage 2972 model system can be further explored in the following ways:

1. Chemical analysis of supernatant isolated after phages kill bacterial cultures using LC-MS. This step would allow us to identify whether the supernatant contains oligopeptides of a size comparable to the peptide we used in the assays and determine their charge, mass, length and sequence.

2. Testing the effect of Pcrap in a semi-solid soft agar environment. As has been shown in other pheromone signalling cascades, bacteria can sometimes

integrate both the information from other cells and environmental stimuli and respond to them only when both inputs are present.

3. Cloning of the *pcraP* sequence on a plasmid under control of an inducible promoter and over expression of the peptide. This should circumvent any difficulties in identification of all possible post-translational modification – the pro-peptide would be expressed in its respective cellular environments with all the modifying enzymes.

4 Conclusions

4.1 Summary of the main results

In this thesis we examined the epidemiological properties of phage spread in bacterial populations in the context of emergence of herd immunity and explored the potential for social immunity.

In Chapter 2 we demonstrated that herd immunity to phages can emerge in bacterial populations. We explored the dynamics of phage spread in structured and unstructured populations consisting of phage-susceptible and phage-resistant individuals and showed that the extent to which herd immunity emerges depends both on population spatial structure and physiology of the hosts. We constructed a mathematical model, which we parametrised using independent experiments and derived predictions for the herd immunity threshold and the velocity of spread of a phage epidemic in a partially resistant population.

In Chapter 3 we explored one potential path bacteria may employ to achieve social immunity. Our results suggest that the potential peptide pheromone, which we identified using bioinformatic analyses and subsequently experimentally tested, may mediate induction of resistance to a phage.

4.2 Maintenance of polymorphism

Bacterial herd immunity may substantially influence eco-evolutionary dynamics in phage-bacterial communities. One of the main consequences of herd immunity is its ability to maintain polymorphism for immunity in the population. In a general deterministic situation, a beneficial allele eventually goes to fixation in a population, but an allele causing resistance to a pathogen can only increase in frequency until it is equal to the herd immunity threshold. Then the pathogen cannot spread in the population anymore and the selection pressure favouring this allele ceases. Thus, once a resistance conferring allele exceeds the herd immunity threshold, it becomes either neutral or selected against, if the immune response is costly. This nature of herd immunity thus generates an evolutionary force, which can generate and maintain polymorphism for immunity in a population. This would not be of much interest if just two morphs would be maintained in a population, but as the diversity of phages is high and bacterial populations are being challenged by more of them simultaneously or sequentially, one can expect that the levels of polymorphism may in the end reach relatively high values. It has been shown that wild populations of bacteria and archaea are highly polymorphic in CRISPR spacer contents (Tyson and Banfield, 2008; Sun *et al.*, 2016; Kuno *et al.*, 2014; Held *et al.*, 2010; Pride *et al.*, 2011; Zhang *et al.*, 2013; Andersson and Banfield, 2008). The authors mostly explain this high polymorphism by rapid simultaneous independent acquisitions of new spacers. In our opinion, this scenario is rather unlikely; we propose that this polymorphism may be rather attributed to herd immunity. It also has been shown that higher diversity in the CRISPR spacer content makes populations more robust to extinction caused by a phage epidemic (van Houte *et al.*, 2016). Therefore, herd immunity may in the end contribute substantially to survival of wild bacterial populations.

4.3 Social immunity

It has been shown that bacteria have evolved many social traits (*i.e.*, population-wide cooperative responses), which result in improved access to nutrients, promoted collective defence against other competitors or increased survival through differentiation, which enables them to better respond to the environment (West *et al.*, 2007; Williams *et al.*, 2007). As phages are presumably a very common threat that bacteria have to face, social immunity fits well into the mosaic of social traits bacteria can express. As a result, social immunity increases the probability of survival of a population by induction of resistance of other members of the population. Although our results are only marginally significant, they show a promising course towards elucidation of a completely new perspective in evolutionary ecology of phage–bacterial communities.

One interesting feature of the signalling peptide we identified is where it is encoded. Its coding sequence is located within a coding sequence of one of the CRISPR/Cas immune system genes, on the antisense strand. As such location of a sequence coding for a signalling molecule has, to our best knowledge, not yet been observed in bacteria, our approach opens a novel framework for a search for signalling molecules involved in other bacterial social traits, or even for other short open reading frames coding for other functional small peptides.

4.4 Future directions

Although this thesis has identified two entirely novel phenomena, herd and social immunity, it provides only the first shards of a mosaic in a new part of evolutionary ecology of phage–bacterial communities. The extent to which these phenomena play a role in nature, however, requires further experimental and theoretical investigations.

As we have pointed out in the introduction, bacteria may possess many various immune systems, whose *modus operandi* differs substantially from the one we

examined. Thus, experimental and theoretical investigation of these other immune systems with respect to their potential to provide herd immunity would help to assess how general this phenomenon might be in nature. Besides investigation of other immune systems, also experimental verification of our prediction that herd immunity may help to maintain polymorphism and promote coexistence of bacteria and phages would extend our understanding of phage–bacterial communities.

Our research on bacterial social immunity, as we have presented it in Chapter 3, surely requires further investigation. First, more tests of bacterial survival upon induction with the signalling peptide and phage infection is necessary. These experiments should be extended to different environments such as soft agar plates, since bacterial quorum sensing is sometimes dependent on other environmental clues. In addition, determination of the charge, mass, length and sequence of peptides isolated form the supernatant using Liquid chromatography–mass spectrometry (LC-MS) can provide further insights into possible post-translational modification of the peptide we identified. Lastly, overexpression of the signalling peptide coding sequence from a plasmid in the wild–type cells would circumvent any difficulties in identification of possible post-translational modification, because the peptide could be accessed by all potentially modifying enzymes.

Bibliography

Stephen T Abedon, *Bacteriophage ecology population growth, evolution, and impact of bacterial viruses*, Cambridge University Press, Cambridge; New York, 2008.

Stephen T Abedon and Rachel R Culler, "Optimizing bacteriophage plaque fecundity," *Journal of theoretical biology*, 249(3):582–592, 2007.

Milton Abramowitz and Irene A Stegun, *Handbook of mathematical functions: with formulas, graphs, and mathematical tables*, volume 55, Courier Corporation, 1964.

Hans-Wolfgang Ackermann, "Phage or Phages," *Bacteriophage*, 1(1):52–53, 2011.

R. M. Anderson, "Evolutionary pressures in the spread and persistence of infectious agents in vertebrate populations," *Parasitology*, 111(S1):S15–S31, 1995.

R. M. Anderson and R. M. May, "Directly transmitted infections diseases: control by vaccination," *Science*, 215(4536):1053–1060, February 1982.

R. M. Anderson and R. M. May, "Spatial, temporal, and genetic heterogeneity in host populations and the design of immunization programmes," *IMA journal of mathematics applied in medicine and biology*, 1(3):233–266, 1984.

R. M. Anderson and R. M. May, "Age-related changes in the rate of disease transmission: implications for the design of vaccination programmes.," *The Journal of Hygiene*, 94(3):365–436, June 1985.

Roy M. Anderson and Robert M. May, "Vaccination and herd immunity to infectious diseases," *, Published online: 28 November 1985; | doi:10.1038/318323a0*, 318(6044):323–329, November 1985.

Roy M. Anderson and Robert M. May, *Infectious Diseases of Humans: Dynamics and Control*, OUP Oxford, August 1992.

Anders F. Andersson and Jillian F. Banfield, "Virus Population Dynamics and Acquired Virus Resistance in Natural Microbial Communities," *Science*, 320(5879):1047–1050, May 2008.

Shea J. Andrews and Joseph A. Rothnagel, "Emerging evidence for functional peptides encoded by short open reading frames," *Nature Reviews Genetics*, 15(3):193–204, March 2014.

Simon A. Babayan and David S. Schneider, "Immunity in Society: Diverse Solutions to Common Problems," *PLOS Biol*, 10(4):e1001297, April 2012.

Rodolphe Barrangou, Christophe Fremaux, Hélène Deveau, Melissa Richards, Patrick Boyaval, Sylvain Moineau, Dennis A. Romero, and Philippe Horvath, "CRISPR Provides Acquired Resistance Against Viruses in Prokaryotes," *Science*, 315(5819):1709–1712, March 2007.

ME Bayer and RW DeBlois, "Diffusion Constant and Dimension of Bacteriophage φX174 as Determined by Self-Beat Laser Light Spectroscopy and Electron Microscopy," *Journal of virology*, 14(4):975–980, 1974.

Joanne Bleackley, Jesse Cooper, Monica Kaminski, and Stephanie Sandilands, "The reduction of T7 phage adsorption in Escherichia coli B23 cells treated with sub-lethal levels of kanamycin," *J Exp Microbiol Immunol*, 13:89–92, 2009.

Robert M. Blumenthal and XIAODONG Cheng, "Restriction-modification systems," *Modern microbial genetics*, pages 177–225, 2002.

B. J. M. Bohannan, B. Kerr, C. M. Jessup, J. B. Hughes, and G. Sandvik, "Trade-offs and coexistence in microbial microcosms," *Antonie Van Leeuwenhoek*, 81(1):107–115, 2002.

B. J. M. Bohannan and R. E. Lenski, "Linking genetic change to community evolution: insights from studies of bacteria and bacteriophage," *Ecology Letters*, 3(4):362–377, 2000.

B. J. M. Bohannan and R. E. Lenski, "The relative importance of competition and predation varies with productivity in a model community," *The American Naturalist*, 156(4):329–340, 2000.

Brendan J. M. Bohannan and Richard E. Lenski, "Effect of Resource Enrichment on a Chemostat Community of Bacteria and Bacteriophage," *Ecology*, 78(8):2303–2315, December 1997.

Brendan J. M. Bohannan and Richard E. Lenski, "Effect of Prey Heterogeneity on the Response of a Model Food Chain to Resource Enrichment.," *The American Naturalist*, 153(1):73–82, January 1999.

Michiel van Boven, Annemarie Bouma, Teun H. F. Fabri, Elly Katsma, Leo Hartog, and Guus Koch, "Herd immunity to Newcastle disease virus in poultry by vaccination," *Avian Pathology*, 37(1):1–5, February 2008.

R Briandet, P Lacroix-Gueu, M Renault, S Lecart, T Meylheuc, E Bidnenko, K Steenkeste, M-N Bellon-Fontaine, and M-P Fontaine-Aupart, "Fluorescence correlation spectroscopy to study diffusion and reaction of bacteriophages inside biofilms," *Applied and environmental microbiology*, 74(7):2135–2143, 2008.

Harald Brüssow, Carlos Canchaya, and Wolf-Dietrich Hardt, "Phages and the evolution of bacterial pathogens: from genomic rearrangements to lysogenic conversion," *Microbiology and molecular biology reviews: MMBR*, 68(3):560–602, table of contents, September 2004.

Angus Buckling and Paul B. Rainey, "Antagonistic coevolution between a bacterium and a bacteriophage," *Proceedings. Biological Sciences*, 269(1494):931–936, May 2002.

Angus Buckling and Paul B. Rainey, "The role of parasites in sympatric and allopatric host diversification," *Nature*, 420(6915):496–499, December 2002.

Andrew Camilli and Bonnie L. Bassler, "Bacterial Small-Molecule Signaling Pathways," *Science*, 311(5764):1113–1116, February 2006.

Mario E Cerritelli, Naiqian Cheng, Alan H Rosenberg, Catherine E McPherson, Frank P Booy, and Alasdair C Steven, "Encapsidated Conformation of Bacteriophage T7 DNA," *Cell*, 91(2):271–280, October 1997.

Chung Cha, Ping Gao, Yu-Ching Chen, Paul D. Shaw, and Stephen K. Farrand, "Production of Acyl-Homoserine Lactone Quorum-Sensing Signals by Gram-Negative Plant-Associated Bacteria," *Molecular Plant-Microbe Interactions*, 11(11):1119–1129, November 1998.

Hélène Chabas, Stineke van Houte, Nina Molin Høyland-Kroghsbo, Angus Buckling, and Edze R Westra, "Immigration of susceptible hosts triggers the evolution of alternative parasite defence strategies," *Proc. R. Soc. B*, 283(1837):20160721, 2016.

Lin Chao, Bruce R. Levin, and Frank M. Stewart, "A Complex Community in a Simple Habitat: An Experimental Study with Bacteria and Phage," *Ecology*, 58(2):369–378, March 1977.

Marie-Christine Chopin, Alain Chopin, and Elena Bidnenko, "Phage abortive infection in lactococci: variations on a theme," *Current Opinion in Microbiology*, 8(4):473–479, August 2005.

Laura C. Cook and Michael J. Federle, "Peptide pheromone signaling in *Streptococcus* and *Enterococcus*," *FEMS Microbiology Reviews*, 38(3):473–492, May 2014.

Jacobus C. de Roode and Thierry Lefèvre, "Behavioral Immunity in Insects," *Insects*, 3(3):789–820, August 2012.

Delphine Destoumieux-Garzón, Sophie Duquesne, Jean Peduzzi, Christophe Goulard, Michel Desmadril, Lucienne Letellier, Sylvie Rebuffat, and Pascale Boulanger, "The iron–siderophore transporter FhuA is the receptor for the antimicrobial peptide microcin J25: role of the microcin Val11–Pro16 β-hairpin

region in the recognition mechanism," *Biochemical Journal*, 389(3):869–876, August 2005.

Hélène Deveau, Rodolphe Barrangou, Josiane E. Garneau, Jessica Labonté, Christophe Fremaux, Patrick Boyaval, Dennis A. Romero, Philippe Horvath, and Sylvain Moineau, "Phage Response to CRISPR-Encoded Resistance in Streptococcus thermophilus," *Journal of Bacteriology*, 190(4):1390–1400, February 2008.

Jennifer A. Doudna and Emmanuelle Charpentier, "The new frontier of genome engineering with CRISPR-Cas9," *Science*, 346(6213):1258096, November 2014.

Martin Duplessis, W. Michael Russell, Dennis A. Romero, and Sylvain Moineau, "Global gene expression analysis of two Streptococcus thermophilus bacteriophages using DNA microarray," *Virology*, 340(2):192–208, September 2005.

Vincent G. H. Eijsink, Lars Axelsson, Dzung B. Diep, Leiv S. Håvarstein, Helge Holo, and Ingolf F. Nes, "Production of class II bacteriocins by lactic acid bacteria; an example of biological warfare and communication," *Antonie van Leeuwenhoek*, 81(1-4):639–654, 2002.

F. Fenner, "Smallpox: emergence, global spread, and eradication," *History and Philosophy of the Life Sciences*, 15(3):397–420, 1993.

M. J Ferrari, S. Bansal, L. A Meyers, and O. N Bjornstad, "Network frailty and the geometry of herd immunity," *Proceedings of the Royal Society B: Biological Sciences*, 273(1602):2743–2748, November 2006.

Noah Fierer and Robert B. Jackson, "The diversity and biogeography of soil bacterial communities," *Proceedings of the National Academy of Sciences of the United States of America*, 103(3):626–631, January 2006.

P. E. Fine, "Herd immunity: history, theory, practice," *Epidemiologic Reviews*, 15(2):265–302, 1993.

Paul Fine, Ken Eames, and David L. Heymann, ""Herd Immunity": A Rough Guide," *Clinical Infectious Diseases*, 52(7):911–916, April 2011.

Ronald A Fisher, "The wave of advance of advantageous genes," *Annals of Human Genetics*, 7(4):355–369, 1937.

Laetitia Fontaine, Céline Boutry, Marie Henry de Frahan, Brigitte Delplace, Christophe Fremaux, Philippe Horvath, Patrick Boyaval, and Pascal Hols, "A Novel Pheromone Quorum-Sensing System Controls the Development of Natural Competence in Streptococcus thermophilus and Streptococcus salivarius," *Journal of Bacteriology*, 192(5):1444–1454, March 2010.

Joaquim Fort and Vicenç Méndez, "Time-delayed spread of viruses in growing plaques," *Physical review letters*, 89(17):178101, 2002.

Joaquim Fort and Vicenç Méndez, "Wavefronts in time-delayed reaction-diffusion systems. Theory and comparison to experiment," *Reports on Progress in Physics*, 65(6):895, 2002.

J. P. Fox, L. Elveback, W. Scott, L. Gatewood, and E. Ackerman, "Herd immunity: basic concept and relevance to public health immunization practices," *American Journal of Epidemiology*, 94(3):179–189, September 1971.

L R García and I J Molineux, "Rate of translocation of bacteriophage T7 DNA across the membranes of Escherichia coli.," *Journal of Bacteriology*, 177(14):4066–4076, July 1995.

Gibson, Wilson, Feil, and Eyre-Walker, "unpublished results," personal communication, 2016.

Tamara Goldfarb, Hila Sberro, Eyal Weinstock, Ofir Cohen, Shany Doron, Yoav Charpak-Amikam, Shaked Afik, Gal Ofir, and Rotem Sorek, "BREX is a novel phage resistance system widespread in microbial genomes," *The EMBO journal*, 34(2):169–183, January 2015.

Nicholas C. Grassly and Christophe Fraser, "Mathematical models of infectious disease transmission," *Nature Reviews Microbiology*, 6(6):477–487, June 2008.

Elisabeth Grohmann, Günther Muth, and Manuel Espinosa, "Conjugative Plasmid Transfer in Gram-Positive Bacteria," *Microbiology and Molecular Biology Reviews*, 67(2):277–301, June 2003.

H Hadas, M Einav, I Fishov, and A Zaritsky, "Bacteriophage T4 development depends on the physiology of its host Escherichia coli," *Microbiology (Reading, England)*, 143 (Pt 1):179–185, January 1997.

Alex R. Hall, Pauline D. Scanlan, Andrew D. Morgan, and Angus Buckling, "Host-parasite coevolutionary arms races give way to fluctuating selection," *Ecology Letters*, 14(7):635–642, July 2011.

Luanne Hall-Stoodley, J. William Costerton, and Paul Stoodley, "Bacterial biofilms: from the Natural environment to infectious diseases," *Nature Reviews Microbiology*, 2(2):95–108, February 2004.

W. H. Hamer, *Epidemic Disease in England: The Evidence of Variability and of Persistency of Type*, Bedford Press, 1906.

A.m.m. Hammad, "Evaluation of alginate-encapsulated Azotobacter chroococcum as a phage-resistant and an effective inoculum," *Journal of Basic Microbiology*, 38(1):9–16, March 1998.

L. S. Håvarstein, P. Gaustad, I. F. Nes, and D. A. Morrison, "Identification of the streptococcal competence-pheromone receptor," *Molecular Microbiology*, 21(4):863–869, August 1996.

J. a. P. Heesterbeek, "A Brief History of R 0 and a Recipe for its Calculation," *Acta Biotheoretica*, 50(3):189–204, September 2002.

Nicole L. Held, Alfa Herrera, Hinsby Cadillo-Quiroz, and Rachel J. Whitaker, "CRISPR Associated Diversity within a Population of Sulfolobus islandicus," *PLoS ONE*, 5(9), September 2010.

Errett C Hobbs, Fanette Fontaine, Xuefeng Yin, and Gisela Storz, "An expanding universe of small proteins," *Current Opinion in Microbiology*, 14(2):167–173, April 2011.

Josef Hofbauer and Karl Sigmund, *Evolutionary games and population dynamics*, Cambridge University Press, 1998.

Philippe Horvath, Dennis A. Romero, Anne-Claire Coûté-Monvoisin, Melissa Richards, Hélène Deveau, Sylvain Moineau, Patrick Boyaval, Christophe Fremaux, and Rodolphe Barrangou, "Diversity, Activity, and Evolution of CRISPR Loci in Streptococcus thermophilus," *Journal of Bacteriology*, 190(4):1401–1412, February 2008.

Laura A. Hug, Brett J. Baker, Karthik Anantharaman, Christopher T. Brown, Alexander J. Probst, Cindy J. Castelle, Cristina N. Butterfield, Alex W. Hernsdorf, Yuki Amano, Kotaro Ise, Yohey Suzuki, Natasha Dudek, David A. Relman, Kari M. Finstad, Ronald Amundson, Brian C. Thomas, and Jillian F. Banfield, "A new view of the tree of life," *Nature Microbiology*, 1:16048, April 2016.

P. Hyman and S. T. Abedon, editors, *Bacteriophages in health and disease*, CABI, Wallingford, 2012, DOI: 10.1079/9781845939847.0000.

Daniel H. Janzen, "When is it Coevolution?," *Evolution*, 34(3):611, May 1980.

Arul Jayaraman and Thomas K. Wood, "Bacterial Quorum Sensing: Signals, Circuits, and Implications for Biofilms and Disease," *Annual Review of Biomedical Engineering*, 10(1):145–167, 2008.

F. Jeltsch, M. S. Müller, V. Grimm, C. Wissel, and R. Brandl, "Pattern formation triggered by rare events: lessons from the spread of rabies," *Proceedings of the Royal Society of London B: Biological Sciences*, 264(1381):495–503, April 1997.

Wenyan Jiang, David Bikard, David Cox, Feng Zhang, and Luciano A. Marraffini, "RNA-guided editing of bacterial genomes using CRISPR-Cas systems," *Nature Biotechnology*, 2013.

Donald A Kaplan, Louis Naumovski, Bruce Rothschild, and R John Collier, "Appendix: a model of plaque formation," *Gene*, 13(3):221–225, 1981.

Emine Kaya, Kevin W. Doxzen, Kilian R. Knoll, Ross C. Wilson, Steven C. Strutt, Philip J. Kranzusch, and Jennifer A. Doudna, "A bacterial Argonaute with noncanonical guide RNA specificity," *Proceedings of the National Academy of Sciences*, 113(15):4057–4062, April 2016.

Helmut Killmann, Georgi Videnov, Gunter Jung, Heinz Schwarz, and Volkmar Braun, "Identification of receptor binding sites by competitive peptide mapping: phages T1, T5, and phi 80 and colicin M bind to the gating loop of FhuA.," *Journal of bacteriology*, 177(3):694–698, 1995.

K. C. King and C. M. Lively, "Does genetic diversity limit disease spread in natural host populations?," *Heredity*, 109(4):199–203, October 2012.

A.N. Kolmogorov, I. Petrovsky, and N. Piscounoff, "Study of the diffusion equation with growth of the quantity of matter and its application to a biology problem," *Bull. Univ. Moscow, Ser. Int. A*, 1(1), 1937.

Matthias Konrad, Meghan L. Vyleta, Fabian J. Theis, Miriam Stock, Simon Tragust, Martina Klatt, Verena Drescher, Carsten Marr, Line V. Ugelvig, and Sylvia Cremer, "Social Transfer of Pathogenic Fungus Promotes Active Immunisation in Ant Colonies," *PLOS Biol*, 10(4):e1001300, April 2012.

Britt Koskella and Michael A. Brockhurst, "Bacteria–phage coevolution as a driver of ecological and evolutionary processes in microbial communities," *FEMS Microbiology Reviews*, 38(5):916–931, September 2014.

Britt Koskella, Derek M. Lin, Angus Buckling, and John N. Thompson, "The costs of evolving resistance in heterogeneous parasite environments," *Proceedings. Biological Sciences*, 279(1735):1896–1903, May 2012.

Sotaro Kuno, Yoshihiko Sako, and Takashi Yoshida, "Diversification of CRISPR within coexisting genotypes in a natural population of the bloom-forming cyanobacterium Microcystis aeruginosa," *Microbiology*, 160(5):903–916, 2014.

S. J. Labrie, J. E. Samson, and S. Moineau, "Bacteriophage resistance mechanisms," *Nature Reviews Microbiology*, 8(5):317–327, 2010.

Richard E. Lenski, "Dynamics of Interactions between Bacteria and Virulent Bacteriophage," In K. C. Marshall, editor, *Advances in Microbial Ecology*, number 10 in Advances in Microbial Ecology, pages 1–44. Springer US, 1988, DOI: 10.1007/978-1-4684-5409-3_1.

Richard E. Lenski and Bruce R. Levin, "Constraints on the Coevolution of Bacteria and Virulent Phage: A Model, Some Experiments, and Predictions for Natural Communities," *The American Naturalist*, 125(4):585–602, April 1985.

Céline Lévesque, Martin Duplessis, Jessica Labonté, Steve Labrie, Christophe Fremaux, Denise Tremblay, and Sylvain Moineau, "Genomic Organization and Molecular Analysis of Virulent Bacteriophage 2972 Infecting an Exopolysaccharide-Producing Streptococcus thermophilus Strain," *Applied and Environmental Microbiology*, 71(7):4057–4068, July 2005.

Bruce R. Levin, Sylvain Moineau, Mary Bushman, and Rodolphe Barrangou, "The Population and Evolutionary Dynamics of Phage and Bacteria with CRISPR–Mediated Immunity," *PLOS Genet*, 9(3):e1003312, March 2013.

Bruce R. Levin, Frank M. Stewart, and Lin Chao, "Resource-Limited Growth, Competition, and Predation: A Model and Experimental Studies with Bacteria and Bacteriophage," *The American Naturalist*, 111(977):3–24, January 1977.

Alun L. Lloyd and Robert M. May, "Spatial Heterogeneity in Epidemic Models," *Journal of Theoretical Biology*, 179(1):1–11, March 1996.

Wil A. M. Loenen, David T. F. Dryden, Elisabeth A. Raleigh, Geoffrey G. Wilson, and Noreen E. Murray, "Highlights of the DNA cutters: a short history of the restriction enzymes," *Nucleic Acids Research*, 42(1):3–19, January 2014.

Meng-Ji Lu and Ulf Henning, "Superinfection exclusion by T-even-type coliphages," *Trends in Microbiology*, 2(4):137 – 139, 1994.

S. E. Luria and M. Delbrück, "Mutations of Bacteria from Virus Sensitivity to Virus Resistance," *Genetics*, 28(6):491–511, November 1943.

Gholson J Lyon and Tom W Muir, "Chemical Signaling among Bacteria and Its Inhibition," *Chemistry & Biology*, 10(11):1007–1021, November 2003.

Gholson J. Lyon and Richard P. Novick, "Peptide signaling in Staphylococcus aureus and other Gram-positive bacteria," *Peptides*, 25(9):1389–1403, September 2004.

Gholson J. Lyon, Jesse S. Wright, Tom W. Muir, and Richard P. Novick, "Key Determinants of Receptor Activation in the agr Autoinducing Peptides of Staphylococcus aureus," *Biochemistry*, 41(31):10095–10104, August 2002.

K. A. Lythgoe and L. Chao, "Mechanisms of coexistence of a bacteria and a bacteriophage in a spatially homogeneous environment," *Ecology Letters*, 6(4):326–334, April 2003.

Charles Mackin, "Quorum Sensing in Archaea," *Honors Scholar Theses*, May 2011.

Erik H. Manting and Arnold JM Driessen, "Escherichia coli translocase: the unravelling of a molecular machine," *Molecular Microbiology*, 37(2):226–238, 2000.

Jeffrey C. Mariner, James A. House, Charles A. Mebus, Albert E. Sollod, Dickens Chibeu, Bryony A. Jones, Peter L. Roeder, Berhanu Admassu, and Gijs G. M. van 't Klooster, "Rinderpest Eradication: Appropriate Technology and Social Innovations," *Science*, 337(6100):1309–1312, September 2012.

Lauren Mashburn-Warren, Donald A. Morrison, and Michael J. Federle, "The Cryptic Competence Pathway in Streptococcus pyogenes Is Controlled by a Peptide Pheromone," *Journal of Bacteriology*, 194(17):4589–4600, September 2012.

Tanja Meister, Helga Lussy, Tamás Bakonyi, Silvie Šikutová, Ivo Rudolf, Wolfgang Vogl, Hans Winkler, Hans Frey, Zdeněk Hubálek, Norbert Nowotny, and Herbert Weissenböck, "Serological evidence of continuing high Usutu virus (Flaviviridae)

activity and establishment of herd immunity in wild birds in Austria," *Veterinary Microbiology*, 127(3–4):237–248, March 2008.

E. Merino, P. Balbás, J. L. Puente, and F. Bolívar, "Antisense overlapping open reading frames in genes from bacteria to humans," *Nucleic Acids Research*, 22(10):1903–1908, May 1994.

J. Meunier, "Social immunity and the evolution of group living in insects," *Philosophical Transactions of the Royal Society B: Biological Sciences*, 370(1669):20140102–20140102, April 2015.

Melissa B. Miller and and Bonnie L. Bassler, "Quorum Sensing in Bacteria," *Annual Review of Microbiology*, 55(1):165–199, 2001.

Namiko Mitarai, Stanley Brown, and Kim Sneppen, "Population dynamics of phage and bacteria in spatially structured habitats using Phage λ and Escherichia coli," *Journal of bacteriology*, 198(12):1783–1793, 2016.

Chihiro Miura, Ken Komatsu, Kensaku Maejima, Takamichi Nijo, Yugo Kitazawa, Tatsuya Tomomitsu, Akira Yusa, Misako Himeno, Kenro Oshima, and Shigetou Namba, "Functional characterization of the principal sigma factor RpoD of phytoplasmas via an in vitro transcription assay," *Scientific Reports*, 5:11893, July 2015.

Akira Murata and Kazuko Kitagawa, "Mechanism of Inactivation of Bacteriophage J1 by Ascorbic Acid," *Agricultural and Biological Chemistry*, 37(5):1145–1151, 1973.

James D Murray, "Mathematical biology I: an introduction, Vol. 17 of interdisciplinary applied mathematics," 2002.

Huong Minh Nguyen and Changwon Kang, "Lysis Delay and Burst Shrinkage of Coliphage T7 by Deletion of Terminator Tφ Reversed by Deletion of Early Genes," *Journal of Virology*, 88(4):2107–2115, February 2014.

D. J. Nokes and R. M. Anderson, "Measles, mumps, and rubella vaccine: what coverage to block transmission?," *The Lancet*, 332(8624):1374, 1988.

Kristina Nordström and Arne Forsgren, "Effect of Protein A on Adsorption of Bacteriophages to Staphylococcus aureus," *Journal of Virology*, 14(2):198–202, August 1974.

Martin A Nowak, *Evolutionary dynamics*, Harvard University Press, 2006.

Pedro H. Oliveira, Marie Touchon, and Eduardo P. C. Rocha, "The interplay of restriction-modification systems with mobile genetic elements and their prokaryotic hosts," *Nucleic Acids Research*, 42(16):10618–10631, September 2014.

Vicente Ortega-Cejas, Joaquim Fort, Vicenç Méndez, and Daniel Campos, "Approximate solution to the speed of spreading viruses," *Physical Review E*, 69(3):031909, 2004.

Mark S. B. Paget and John D. Helmann, "The sigma70 family of sigma factors," *Genome Biology*, 4(1):203, 2003.

Zeev Pancer and Max D. Cooper, "The Evolution of Adaptive Immunity," *Annual Review of Immunology*, 24(1):497–518, 2006.

Matthew R. Parsek and E. P. Greenberg, "Sociomicrobiology: the connections between quorum sensing and biofilms," *Trends in Microbiology*, 13(1):27–33, January 2005.

Marta Perego, Philippe Glaser, and James A. Hoch, "Aspartyl-phosphate phosphatases deactivate the response regulator components of the sporulation signal transduction system in Bacillus subtilis," *Molecular Microbiology*, 19(6):1151–1157, March 1996.

Thomas Nordahl Petersen, Søren Brunak, Gunnar von Heijne, and Henrik Nielsen, "SignalP 4.0: discriminating signal peptides from transmembrane regions," *Nature Methods*, 8(10):785–786, October 2011.

David T. Pride, Christine L. Sun, Julia Salzman, Nitya Rao, Peter Loomer, Gary C. Armitage, Jillian F. Banfield, and David A. Relman, "Analysis of streptococcal CRISPRs from human saliva reveals substantial sequence diversity within and between subjects over time," *Genome Research*, 21(1):126–136, January 2011.

James I. Prosser, Brendan J. M. Bohannan, Tom P. Curtis, Richard J. Ellis, Mary K. Firestone, Rob P. Freckleton, Jessica L. Green, Laura E. Green, Ken Killham, Jack J. Lennon, A. Mark Osborn, Martin Solan, Christopher J. van der Gast, and J. Peter W. Young, "The role of ecological theory in microbial ecology," *Nature Reviews Microbiology*, 5(5):384–392, May 2007.

Luis E. N. Quadri, "Regulation of antimicrobial peptide production by autoinducer-mediated quorum sensing in lactic acid bacteria," *Antonie van Leeuwenhoek*, 82(1-4):133–145, 2002.

Leslie A. Real and Roman Biek, "Spatial dynamics and genetics of infectious diseases on heterogeneous landscapes," *Journal of The Royal Society Interface*, 4(16):935–948, October 2007.

Jorge Rocha-Estrada, Angel E. Aceves-Diez, Gabriel Guarneros, and Mayra de la Torre, "The RNPP family of quorum-sensing proteins in Gram-positive bacteria," *Applied Microbiology and Biotechnology*, 87(3):913–923, May 2010.

Steven T. Rutherford and Bonnie L. Bassler, "Bacterial Quorum Sensing: Its Role in Virulence and Possibilities for Its Control," *Cold Spring Harbor Perspectives in Medicine*, 2(11):a012427, November 2012.

Dieter Schenzle, "An Age-Structured Model of Pre- and Post-Vaccination Measles Transmission," *Mathematical Medicine and Biology*, 1(2):169–191, January 1984.

S. J. Schrag and J. E. Mittler, "Host-Parasite Coexistence: The Role of Spatial Refuges in Stabilizing Bacteria-Phage Interactions," *The American Naturalist*, 148(2):348–377, August 1996.

V Solovyev and A Salamov, "Automatic Annotation of Microbial Genomes and Metagenomic Sequences (Ed. R.W. Li), Nova Science Publishers, p.61-78.," In R.W. Li, editor, *Metagenomics and its Applications in Agriculture, Biomedicine and Environmental Studies*, pages 61–78. Nova Science Publishers, 2011.

H. E. Soper, “The Interpretation of Periodicity in Disease Prevalence,” *Journal of the Royal Statistical Society*, 92(1):34–73, 1929.

Rotem Sorek, C. Martin Lawrence, and Blake Wiedenheft, “CRISPR-Mediated Adaptive Immune Systems in Bacteria and Archaea,” *Annual Review of Biochemistry*, 82(1):237–266, 2013.

Elisabeth Steiner, Jamie Scott, Nigel P. Minton, and Klaus Winzer, “An agr Quorum Sensing System That Regulates Granulose Formation and Sporulation in Clostridium acetobutylicum,” *Applied and Environmental Microbiology*, 78(4):1113–1122, February 2012.

Gunther S Stent and Elie L Wollman, “On the two-step nature of bacteriophage adsorption,” *Biochimica et biophysica acta*, 8:260–269, 1952.

Adi Stern and Rotem Sorek, “The phage-host arms-race: Shaping the evolution of microbes,” *Bioessays*, 33(1):43–51, January 2011.

Christine L. Sun, Brian C. Thomas, Rodolphe Barrangou, and Jillian F. Banfield, “Metagenomic reconstructions of bacterial CRISPR loci constrain population histories,” *The ISME journal*, 10(4):858–870, 2016.

Ian W Sutherland, Kevin A Hughes, Lucy C Skillman, and Karen Tait, “The interaction of phage and biofilms,” *FEMS microbiology letters*, 232(1):1–6, 2004.

Daan C. Swarts, Matthijs M. Jore, Edze R. Westra, Yifan Zhu, Jorijn H. Janssen, Ambrosius P. Snijders, Yanli Wang, Dinshaw J. Patel, José Berenguer, Stan J. J. Brouns, and John van der Oost, “DNA-guided DNA interference by a prokaryotic Argonaute,” *Nature*, 507(7491):258–261, March 2014.

Tian Tian and Howard M. Salis, “A predictive biophysical model of translational coupling to coordinate and control protein expression in bacterial operons,” *Nucleic Acids Research*, page gkv635, June 2015.

Gene W. Tyson and Jillian F. Banfield, “Rapidly evolving CRISPRs implicated in acquired resistance of microorganisms to viruses,” *Environmental Microbiology*, 10(1):200–207, January 2008.

Stineke van Houte, Alice K. E. Ekroth, Jenny M. Broniewski, Hélène Chabas, Ben Ashby, Joseph Bondy-Denomy, Sylvain Gandon, Mike Boots, Steve Paterson, Angus Buckling, and Edze R. Westra, "The diversity-generating benefits of a prokaryotic adaptive immune system," *Nature*, 532(7599):385–388, April 2016.

Wim van Saarloos, "Front propagation into unstable states," *Physics reports*, 386(2):29–222, 2003.

Leigh Van Valen, "A new evolutionary law," *Evolutionary theory*, 1:1–30, 1973.

M. K. Waldor and J. J. Mekalanos, "Lysogenic conversion by a filamentous phage encoding cholera toxin," *Science (New York, N.Y.)*, 272(5270):1910–1914, June 1996.

Yundan Wang, Pengcheng Yang, Feng Cui, and Le Kang, "Altered Immunity in Crowded Locust Reduced Fungal (Metarhizium anisopliae) Pathogenesis," *PLOS Pathog*, 9(1):e1003102, January 2013.

Joshua S Weitz, *Quantitative Viral Ecology: Dynamics of Viruses and Their Microbial Hosts*, Princeton University Press, 2016.

Stuart A. West, Stephen P. Diggle, Angus Buckling, Andy Gardner, and Ashleigh S. Griffin, "The Social Lives of Microbes," *Annual Review of Ecology, Evolution, and Systematics*, 38:53–77, 2007.

Edze R Westra, Stineke van Houte, Sam Oyesiku-Blakemore, Ben Makin, Jenny M Broniewski, Alex Best, Joseph Bondy-Denomy, Alan Davidson, Mike Boots, and Angus Buckling, "Parasite exposure drives selective evolution of constitutive versus inducible defense," *Current Biology*, 25(8):1043–1049, 2015.

William B. Whitman, David C. Coleman, and William J. Wiebe, "Prokaryotes: The unseen majority," *Proceedings of the National Academy of Sciences*, 95(12):6578–6583, June 1998.

Paul Williams, Klaus Winzer, Weng C. Chan, and Miguel Cámara, "Look who's talking: communication and quorum sensing in the bacterial world," *Philosophical*

Transactions of the Royal Society of London. Series B, Biological Sciences, 362(1483):1119–1134, July 2007.

Christopher Wills and Douglas R Green, "A Genetic Herd-Immunity Model for the Maintenance of MHC Polymorphism," *Immunological reviews*, 143(1):263–292, 1995.

Kenneth Wilson, Robert Knell, Michael Boots, and Jane Koch-Osborne, "Group living and investment in immune defence: an interspecific analysis," *Journal of Animal Ecology*, 72(1):133–143, January 2003.

John Yin and JS McCaskill, "Replication of viruses in a growing plaque: a reaction-diffusion model.," *Biophysical journal*, 61(6):1540, 1992.

J. A. Yorke, N. Nathanson, G. Pianigiani, and J. Martin, "Seasonality and the requirements for perpetuation and eradication of viruses in populations," *American Journal of Epidemiology*, 109(2):103–123, February 1979.

Lingchong You and John Yin, "Amplification and spread of viruses in a growing plaque," *Journal of theoretical biology*, 200(4):365–373, 1999.

Quan Zhang, Mina Rho, Haixu Tang, Thomas G. Doak, and Yuzhen Ye, "CRISPR-Cas systems target a diverse collection of invasive mobile genetic elements in human microbiomes," *Genome Biology*, 14:R40, 2013.